E. Wolf, Progress in Optics 42

Chapter 3

Quantum Zeno and inverse quantum Zeno effects

by

Paolo Facchi and Saverio Pascazio

Dipartimento di Fisica, Università di Bari and
Istituto Nazionale di Fisica Nucleare, Sezione di Bari, 70126 Bari, Italy

Contents

§ 1. Introduction

Zeno and his master Parmenides lived about 2500 years ago in Elea, a small Italian town not far from Naples, in the Mediterranean region called "Magna Graecia". Parmenides, a profound and innovative philosopher, believed that senses are deceptive and our perception of reality in continuous change is an illusion. In his conception, there is a unique, indivisible *Truth* ("being") that does not undergo any change ("becoming") and cannot be decomposed into smaller entities. Zeno was Parmenides' most brilliant disciple and in order to support his master's ideas he would challenge the most "obvious" conclusions of common sense by putting forward many paradoxical examples. His captious arguments are ingenious and very famous. For example, he argued that Achilles, who starts running from point A, cannot reach a turtle that at the same time starts moving from point B, because when the former reaches B the latter has moved to C, and so on *ad infinitum*. Against the very idea of dividing an object into parts, he claimed that if a finite segment is made up of an infinite number of points then one runs into a contradictory conclusion: indeed, if a single point has a finite size, then the size of the segment is infinite; if, on the other hand, a single point has no size, their sum (the segment itself) cannot have a nonvanishing size.

Zeno lacked the concept of *infinitesimal*. Modern infinitesimal calculus resolves the first paradox by introducing the concept of velocity as the derivative of position with respect to time: Achilles will reach the turtle in a *finite* time because it takes a very small time to cover a very small distance, where "very small" times and distances are infinitesimal of the same order. The solution of the second paradox is even subtler. An *uncountable* ensemble of points can have a *nonvanishing* size. At any rate, it is undeniable that his provocative arguments foreran very subtle concepts of infinitesimal calculus, such as derivatives, Riemann and Lebesgue measures. More to this, one should not forget that Zeno aimed at challenging the "obviousness" of common sense, in order to support the philosophy of his master Parmenides and bring to light the difficulties inherent in the very idea of "becoming".

One of Zeno's paradoxes will be the object of the present investigation: A sped arrow never reaches its target, because at every instant of time, if we look at the arrow, we see that it occupies a portion of space equal to its own size. At any

given moment the arrow is therefore immobile, and by summing up many such "immobilities" it is clearly impossible, according to Zeno, to obtain motion. It is amusing that some quantum-mechanical states, under particular conditions, behave in a way that is reminiscent of this paradox.

In this chapter we shall review the main features of the so-called quantum Zeno effect (von Neumann [1932], Beskow and Nilsson [1967], Khalfin [1968], Misra and Sudarshan [1977]). In very few words, the evolution of a quantum-mechanical state can be slowed down (or even halted in some limit) when very frequent measurements are performed on the system, in order to check whether it is still in its initial state: Zeno's quantum arrow (the wave function) does not move, if it is continuously observed.

The interest in the quantum Zeno effect (QZE) has been revived, during the last decade, mainly because of some interesting proposals that made it liable to *experimental* investigation. Unlike previous studies, confined to a purely academic level, the investigation of the last few years has focused on practical experiments, possible applications, as well as theoretical implications and interpretative issues. In this chapter we shall first review the main features of the QZE and discuss some simple examples. We shall then concentrate our attention on more interesting physical situations and emphasize the occurrence of new physical phenomena, such as the "inverse" quantum Zeno effect.

The quantum Zeno effect has been mainly investigated for oscillating systems (Cook [1988], Itano, Heinzen, Bollinger and Wineland [1990], Pascazio, Namiki, Badurek and Rauch [1993], Kwiat, Weinfurter, Herzog, Zeilinger and Kasevich [1995], Luis and Peřina [1996]), whose Poincaré time is finite. However, the discussion cannot be limited to oscillating systems. New and somewhat unexpected phenomena are disclosed when one considers unstable systems, whose Poincaré time is infinite (Bernardini, Maiani and Testa [1993], Facchi and Pascazio [1998], Maiani and Testa [1998], Joichi, Matsumoto and Yoshimura [1998], Alvarez-Estrada and Sánchez-Gómez [1999]). Unfortunately, in this case the analysis becomes more complicated and requires a quantum field theoretical framework. The QZE has recently become such a wide subject of investigation, that it is difficult to discuss all its multiple facets. In this chapter we shall therefore discuss only some of its aspects, by focusing our attention on quantum optics and quantum electrodynamics. As a general philosophy, we shall always start by considering simple physical systems and then extend our analysis to more complicated cases. As already emphasized, it would be wrong to limit the analysis to elementary situations (such as oscillating systems), because in doing so one would overlook a great deal of interesting physical effects. We will

therefore try to follow Einstein's precept: Things should be made as simple as possible, but not simpler.

In this chapter we will often work in natural units ($\hbar = c = 1$), but will put the physical constants back in the final formulas whenever it will be helpful to get a feeling for the numbers. After setting up the notation in § 2, we introduce in § 3 the fundamentals of the quantum Zeno and "inverse" quantum Zeno effect (IZE), by making use of elementary quantum-mechanical techniques. We shall first use the seminal formulation of QZE in terms of projection operators: This is the usual approach and makes use of what we might call a "pulsed" observation of the quantum state (Mihokova, Pascazio and Schulman [1997], Schulman [1998]). We then explain in § 4 that it is not necessary to use projection operators and nonunitary dynamics. A fully dynamical explanation of the QZE is possible, involving Hamiltonians and no projectors (Pascazio and Namiki [1994], Petrosky, Tasaki and Prigogine [1990]). In § 5 we introduce the notion of "continuous" observation of the quantum state, e.g., performed by means of an intense field. Although this idea has been revived only recently (Mihokova, Pascazio and Schulman [1997], Schulman [1998]), it is contained, in embryo, in earlier papers (Kraus [1981], Peres [1980], Plenio, Knight and Thompson [1996]). This idea will lead us to a novel definition of QZE in § 6. We then discuss, in § 7, an interesting example of QZE in quantum optics, both with pulsed and continuous measurements. We look at a down-conversion process in a nonlinear crystal as a "decay" of a pump photon into a pair of signal and idler photons of lower frequency and study how the "decay" is modified by a measurement process of some sort. Interestingly, this system discloses the presence of an inverse Zeno effect. We shall see that by increasing the strength of the observation, the "decay" is sometimes accelerated rather than hindered. In § 8 we consider the QZE and IZE for *bona fide* unstable systems. This is a more complicated problem, because it requires the use of quantum field theoretical techniques. The study of a solvable (but significant) example enables us to understand the role played by the Weisskopf–Wigner approximation (Gamow [1928], Weisskopf and Wigner [1930a,b], Breit and Wigner [1936]) and the Fermi "golden rule" (Fermi [1932, 1950, 1960]). Moreover, we shall see that for an unstable system, the form factors of the interaction play a fundamental role and determine the occurrence of a Zeno or an inverse Zeno regime, depending on the physical parameters describing the system. We finally investigate, in § 9, the intriguing possibility that the lifetime of an unstable quantum system be modified by the presence of a very intense electromagnetic field. We shall look at the temporal behavior of a three-level system (such as an atom or a molecule) illuminated by an intense laser field (Pascazio and Facchi [1999], Facchi and Pascazio [2000]) and see

that, for physically sensible values of the intensity of the laser, the decay can be *enhanced*. This will be interpreted as an inverse quantum Zeno effect.

The choice of the subjects that appear in this review article reflects our own point of view on the quantum Zeno problem. This was inevitable and requires an apology. Some important aspects of this problem were either left out or only briefly mentioned. We regret, in particular, that some very important features of the temporal evolution, arising from a genuine quantum field theoretical analysis, are not even mentioned. Moreover, we will not explore other very important topics, such as neutron physics, irreversibility and deviations from Markovianity. On the other hand, we intentionally did not discuss some academic issues of no practical interest.

We shall not look in detail at the characteristics of the quantum-mechanical evolution law at short times (Beskow and Nilsson [1967], Khalfin [1968], Wilkinson, Bharucha, Fischer, Madison, Morrow, Niu, Sundaram and Raizen [1997]) and long times (Mandelstam and Tamm [1945], Fock and Krylov [1947], Hellund [1953], Namiki and Mugibayashi [1953], Khalfin [1957, 1958]). These are summarized in Nakazato, Namiki and Pascazio [1996] and will often be taken for granted. An excellent account of the most recent results on the QZE can be found in Home and Whitaker [1997] and Whitaker [2000].

Our attention will mainly be focused on quantum optics and quantum electrodynamics. Specific examples will be given particular importance and will therefore play a fundamental role. We will not attempt to generalize, unless necessary. The *leitmotif* of this chapter is that the quantum Zeno effect is a dynamical phenomenon, that can be explained in terms of the Schrödinger equation, without making use of projection operators. We will implicitly assume, throughout our discussion, that a projection operator is just a shorthand notation that summarizes the effects of a much more complicated underlying dynamical process, involving a huge number of elementary quantum-mechanical systems (Namiki, Pascazio and Nakazato [1997]). This idea will constitute the "backbone" of our work. Only if this concept is fully elaborated and completely digested, can one realize that a broader definition of Zeno effect is required, that takes into account the very concept of continuous measurement, performed for example by a quantum field.

§ 2. Two-level systems and Bloch vector

We start by considering a two-level system undergoing Rabi oscillations. This is the simplest nontrivial quantum-mechanical example, for it involves 2×2

matrices and very simple algebra. One can think of an atom illuminated by a laser field whose frequency resonates with one of the atomic transitions, or a neutron spin in a magnetic field. We shall neglect the energy difference between the two states $|\pm\rangle$. The (interaction) Hamiltonian reads

$$H_{\rm I} = \Omega\sigma_1 = \Omega(|+\rangle\langle -| + |-\rangle\langle +|) = \begin{pmatrix} 0 & \Omega \\ \Omega & 0 \end{pmatrix}, \tag{2.1}$$

where Ω is a real number, σ_j ($j = 1,2,3$) the Pauli matrices and

$$|+\rangle = \begin{pmatrix} 1 \\ 0 \end{pmatrix}, \quad |-\rangle = \begin{pmatrix} 0 \\ 1 \end{pmatrix} \tag{2.2}$$

are eigenstates of σ_3. We will use the above notation interchangeably. Let the initial state be

$$|\psi_0\rangle = |+\rangle = \begin{pmatrix} 1 \\ 0 \end{pmatrix}, \tag{2.3}$$

so that the evolution yields

$$|\psi_t\rangle = e^{-{\rm i}H_{\rm I}t}|\psi_0\rangle = \cos(\Omega t)|+\rangle - {\rm i}\sin(\Omega t)|-\rangle = \begin{pmatrix} \cos\Omega t \\ -{\rm i}\sin\Omega t \end{pmatrix}. \tag{2.4}$$

In the following, we shall often make use of the rotating coordinates, introduced by Bloch [1946] and Rabi, Ramsey and Schwinger [1954], and of well-known computational techniques due to Feynman, Vernon and Hellwarth [1957]. In terms of the polarization (Bloch) vector

$$\boldsymbol{R}(t) = \langle\psi_t|\boldsymbol{\sigma}|\psi_t\rangle = (R_1, R_2, R_3)^{\rm T}, \tag{2.5}$$

where $^{\rm T}$ denotes the transposed matrix, the Schrödinger equation reads

$$\dot{\boldsymbol{R}}(t) = 2\boldsymbol{\Omega} \times \boldsymbol{R}(t), \tag{2.6}$$

where

$$\boldsymbol{\Omega} = (\Omega, 0, 0)^{\rm T}. \tag{2.7}$$

The norm of the Bloch vector is preserved: $\|\boldsymbol{R}(t)\| = 1, \forall t$. See fig. 1.

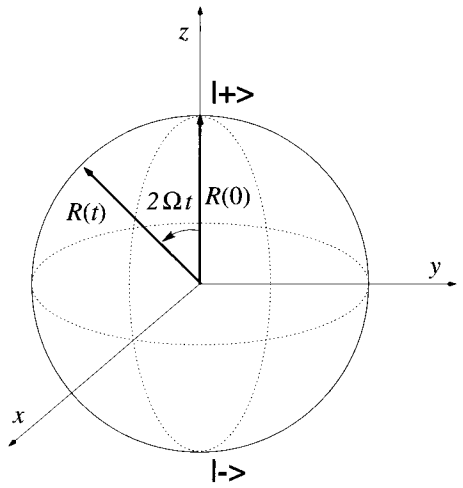

The density matrix of a two-level system is expressed in terms of the Bloch vector according to the formula

$$\rho = \begin{pmatrix} \rho_{++} & \rho_{+-} \\ \rho_{-+} & \rho_{--} \end{pmatrix} = \tfrac{1}{2}(\mathbf{1} + \boldsymbol{R}\cdot\boldsymbol{\sigma}), \tag{2.8}$$

so that

$$\begin{aligned} \rho_{\pm\pm} &= \tfrac{1}{2}(1 \pm R_3) = P_{\pm}, \\ \rho_{\pm\mp} &= \tfrac{1}{2}(R_1 \mp \mathrm{i}R_2), \end{aligned} \tag{2.9}$$

where $P_{\pm} \equiv \rho_{\pm\pm}$ is the probability that the system is in level $\pm$. Notice that $\mathrm{Tr}\,\rho = P_+ + P_- = 1$ (normalization) and $\mathrm{Tr}(\rho\boldsymbol{\sigma}) = \boldsymbol{R}$. Vice versa, the Bloch vector is readily expressed in terms of the density matrix:

$$\begin{aligned} R_1 &= \rho_{+-} + \rho_{-+}, \\ R_2 &= \mathrm{i}(\rho_{+-} - \rho_{-+}), \\ R_3 &= \rho_{++} - \rho_{--} = P_+ - P_-. \end{aligned} \tag{2.10}$$

The level configuration and the dynamics of the oscillations are shown in fig. 2. Observe that the probability returns to its initial value after a time $T_{\mathrm{P}} = \pi/\Omega$. This is a very simple instance of Poincaré recurrence time.

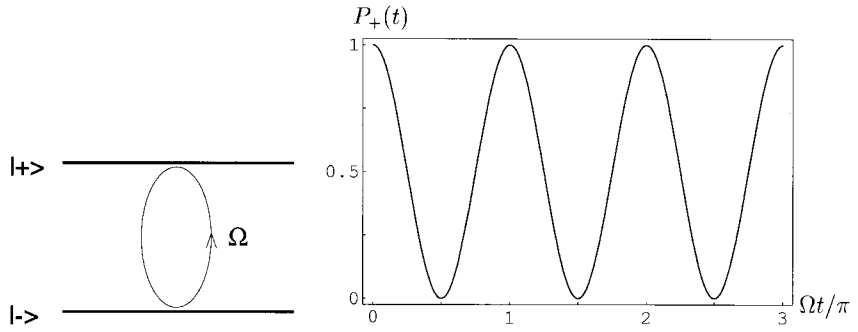

Fig. 2. Rabi oscillations in a two-level system.

§ 3. Pulsed observation

Let us introduce the fundamental features of the quantum Zeno effect. We shall follow the "historical" approach (von Neumann [1932], Beskow and Nilsson [1967], Khalfin [1968], Misra and Sudarshan [1977]), by considering "pulsed" measurements. The alternative notion of continuous measurement will be discussed in § 5.

For the sake of simplicity we shall often refer to two-level systems. This will make our analysis more transparent. It goes without saying that more general and formal approaches are also possible (Nakazato, Namiki and Pascazio [1996], Home and Whitaker [1997]).

3.1. *Survival probability under pulsed measurements*

We define the *survival amplitude*

$$\mathcal{A}(t) = \langle\psi_0|\psi_t\rangle = \langle\psi_0|\mathrm{e}^{-\mathrm{i}Ht}|\psi_0\rangle \tag{3.1}$$

and the *survival probability*

$$P(t) = |\mathcal{A}(t)|^2 = |\langle\psi_0|\mathrm{e}^{-\mathrm{i}Ht}|\psi_0\rangle|^2, \tag{3.2}$$

where H is the total Hamiltonian of the system. These quantities represent the amplitude and probability that a quantum system, initially prepared in state $|\psi_0\rangle$, is still in the same state at time t. An elementary expansion shows that the behavior of the survival probability at short times is quadratic

$$P(t) = 1 - t^2/\tau_{\mathrm{Z}}^2 + \cdots, \qquad \tau_{\mathrm{Z}}^{-2} \equiv \langle\psi_0|H^2|\psi_0\rangle - \langle\psi_0|H|\psi_0\rangle^2. \tag{3.3}$$

For instance, with the Hamiltonian (2.1) one finds

$$\mathcal{A}(t) = \cos\Omega t, \tag{3.4}$$

$$P(t) = \cos^2 \Omega t, \tag{3.5}$$

$$\tau_Z = \Omega^{-1}. \tag{3.6}$$

The quantity τ_Z is the "Zeno time" and seemingly yields a quantitative estimate of the short-time behavior. As we shall see in this chapter, this is a *misleading estimate* in many situations. Strictly speaking, τ_Z is simply the convexity of $P(t)$ in the origin. Note that if one writes

$$H = H_0 + H_1, \qquad \text{with} \quad H_0|\psi_0\rangle = \omega_0|\psi_0\rangle, \quad \langle\psi_0|H_1|\psi_0\rangle = 0, \tag{3.7}$$

the Zeno time reads

$$\tau_Z^{-2} = \langle\psi_0|H_1^2|\psi_0\rangle. \tag{3.8}$$

Therefore τ_Z depends only on the square of the off-diagonal part of the Hamiltonian.

Let us now perform N measurements at time intervals τ, in order to check whether the system is still in its initial state. The survival probability after the measurements reads

$$P^{(N)}(t) = P(\tau)^N = P\left(\frac{t}{N}\right)^N \simeq \left[1 - \left(\frac{t}{N\tau_Z}\right)^2\right]^N \overset{N \text{ large}}{\longrightarrow} \exp\left(-\frac{t^2}{N\tau_Z^2}\right) \overset{N\to\infty}{\longrightarrow} 1, \tag{3.9}$$

where $t = N\tau$ is the total duration of the experiment. The $N \to \infty$ limit was originally named limit of "continuous observation" and regarded as a paradoxical result (Misra and Sudarshan [1977]): Infinitely frequent measurements halt the quantum-mechanical evolution and "freeze" the system in its initial state. Zeno's quantum-mechanical arrow (the wave function), sped by the Hamiltonian, does not move, if it is continuously observed. The investigation of the last few years has shown that the QZE is not paradoxical. Although the $N \to \infty$ limit must be considered as a mathematical abstraction (Ghirardi, Omero, Weber and Rimini [1979], Nakazato, Namiki, Pascazio and Rauch [1995], Venugopalan and Ghosh [1995], Pati [1996], Hradil, Nakazato, Namiki, Pascazio and Rauch [1998]), the evolution of a quantum system can indeed be slowed down for sufficiently large N (Itano, Heinzen, Bollinger and Wineland [1990], Petrosky, Tasaki and Prigogine [1990, 1991], Peres and Ron [1990], Ballentine [1991], Itano, Heinzen, Bollinger and Wineland [1991], Frerichs and Schenzle [1992], Inagaki, Namiki and Tajiri [1992], Home and Whitaker [1992, 1993], Pascazio, Namiki, Badurek and Rauch [1993], Blanchard and Jadczyk [1993], Altenmuller and Schenzle

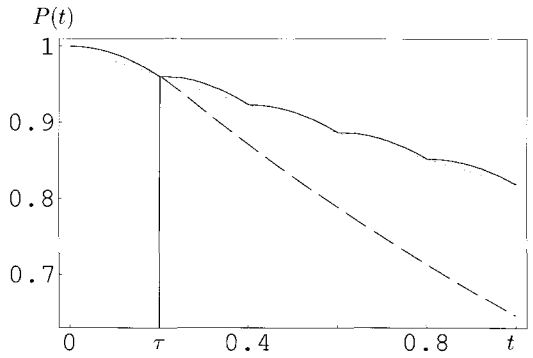

Fig. 3. Evolution with frequent "pulsed" measurements: quantum Zeno effect. The dashed (solid) line is the survival probability without (with) measurements.

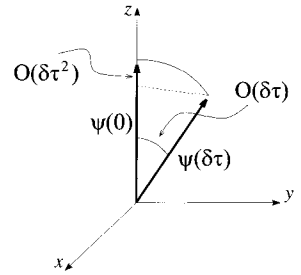

Fig. 4. Short-time evolution of phase and probability.

[1994], Pascazio and Namiki [1994], Schulman, Ranfagni and Mugnai [1994], Berry [1995], Beige and Hegerfeldt [1996], Kofman and Kurizki [1996], Schulman [1997], Thun and Peřina [1998]). The Zeno evolution is shown in fig. 3.

In a few words, the QZE is ascribable to the following mathematical properties of the Schrödinger equation. In a short time $\delta\tau \sim 1/N$, the phase of the wave function evolves like $O(\delta\tau)$, while the probability changes by $O(\delta\tau^2)$, so that

$$P^{(N)}(t) \simeq \left[1 - O(1/N^2)\right]^N \overset{N\to\infty}{\longrightarrow} 1. \tag{3.10}$$

This is sketched in fig. 4; it is a very general feature of the Schrödinger equation.

3.2. *Quantum Zeno and Inverse quantum Zeno effects*

It is convenient to rewrite eq. (3.9) in the following way ($t = N\tau$)

$$P^{(N)}(t) = P(\tau)^N = \exp(N \log P(\tau)) = \exp(-\gamma_{\text{eff}}(\tau)t), \tag{3.11}$$

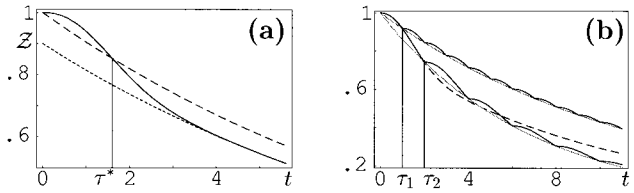

Fig. 5. (a) Determination of τ^*. The solid line is the survival probability, the dashed line is the exponential $e^{-\gamma t}$, and the dotted line is the asymptotic exponential $\mathcal{Z}e^{-\gamma t}$ in eq. (3.17). (b) Quantum Zeno vs. inverse Zeno ("Heraclitus") effect. The dashed line represents a typical behavior of the survival probability $P(t)$ when no measurement is performed: the short-time Zeno region is followed by an approximately exponential decay with a natural decay rate γ. When measurements are performed at time intervals τ, we get the effective decay rate $\gamma_{\text{eff}}(\tau)$. The solid lines represent the survival probabilities, and the dotted lines their exponential interpolations, according to eq. (3.11). For $\tau_1 < \tau^* < \tau_2$ the effective decay rate $\gamma_{\text{eff}}(\tau_1)$ [$\gamma_{\text{eff}}(\tau_2)$] is smaller (QZE) [larger (IZE)] than the "natural" decay rate γ. When $\tau = \tau^*$ one recovers the natural lifetime, according to eq. (3.15).

where we introduced an effective decay rate

$$\gamma_{\text{eff}}(\tau) \equiv -\frac{1}{\tau}\log P(\tau). \tag{3.12}$$

For instance, for times τ such that $P(\tau) \simeq \exp(-\tau^2/\tau_Z^2)$ with good approximation, one easily checks that γ_{eff} is a linear function of τ

$$\gamma_{\text{eff}}(\tau) \sim \frac{\tau}{\tau_Z^2}, \qquad \text{for} \quad \tau \to 0. \tag{3.13}$$

Notice that $\gamma_{\text{eff}}(\tau)$ in eq. (3.12) represents the effective decay rate of a system that evolves freely up to time τ and is measured at time τ. One expects to recover the "natural" decay rate γ (if it exists), in agreement with the Fermi "golden" rule, for sufficiently long times, i.e., after the initial quadratic region is over

$$\gamma_{\text{eff}}(\tau) \overset{\text{"long"}\ \tau}{\longrightarrow} \gamma. \tag{3.14}$$

The *quantitative* meaning of the expression "long" in the above equation represents an interesting conceptual problem and will be tackled in § 8. Suffice it to say, at this stage, that τ_Z is not the right time scale.

We now concentrate our attention on a truly unstable system, with decay rate γ. We ask whether it is possible to find a finite time τ^* such that

$$\gamma_{\text{eff}}(\tau^*) = \gamma. \tag{3.15}$$

If such a time exists, then by performing measurements at time intervals τ^* the system decays according to its "natural" lifetime, as if no measurements were performed. By eqs. (3.15) and (3.12) one gets

$$P(\tau^*) = e^{-\gamma\tau^*}, \tag{3.16}$$

i.e., τ^* is the intersection between the curves $P(t)$ and $e^{-\gamma t}$. Figure 5 illustrates

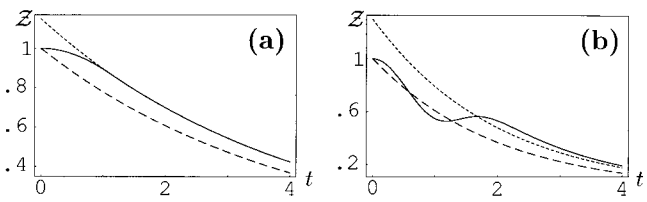

Fig. 6. Study of the case $\mathcal{Z} > 1$. The solid line is the survival probability, the dashed line is the renormalized exponential $e^{-\gamma t}$, and the dotted line is the asymptotic exponential $\mathcal{Z}e^{-\gamma t}$. (a) If $P(t)$ and $e^{-\gamma t}$ do not intersect, then no finite solution τ^* exists. (b) If $P(t)$ and $e^{-\gamma t}$ intersect, then a finite solution τ^* exists. (In this case there are always at least two intersections.)

an example in which such a time τ^* exists. By looking at this figure, it is evident that if $\tau = \tau_1 < \tau^*$ one obtains a QZE. *Vice versa*, if $\tau = \tau_2 > \tau^*$, one obtains an *inverse* Zeno effect (IZE). In this sense, τ^* can be viewed as a *transition time* from a quantum Zeno to an inverse Zeno effect. Paraphrasing Misra and Sudarshan (Misra and Sudarshan [1977]) we can say that τ^* determines the transition from Zeno (who argued that a sped arrow, if observed, does not move) to Heraclitus (who replied that everything flows). We shall see that in general it is not always possible to determine τ^*: eq. (3.15) may have no finite solutions. This will be thoroughly discussed in the following, but it is interesting to anticipate some general conclusions. As we shall see in §§ 7 and 8, for an unstable system and for sufficiently "long" times (the definition of "long" times will be sharpened later) the survival probability reads with very good approximation

$$P(t) = |\mathcal{A}(t)|^2 \simeq \mathcal{Z}e^{-\gamma t}, \tag{3.17}$$

where $\mathcal{Z}$, the intersection of the asymptotic exponential with the $t = 0$ axis, is the wave function renormalization and is given by the square modulus of the residue of the pole of the propagator. We claim that a sufficient condition for the existence of a solution τ^* of eq. (3.15) is that $\mathcal{Z} < 1$. This is easily proved by graphical inspection. The case $\mathcal{Z} < 1$ is shown in fig. 5a: $P(t)$ and $e^{-\gamma t}$ must intersect, since according to (3.17) $P(t) \sim \mathcal{Z}e^{-\gamma t}$ for large t, and a finite solution τ^* can always be found. The other case, $\mathcal{Z} > 1$, is shown in fig. 6. A solution may or may not exist, depending on the features of the model investigated. We shall come back to the Zeno–Heraclitus transition in §§ 7 and 8. The occurrence of an inverse Zeno effect has been discussed by several authors, in different contexts (Pascazio [1996], Schulman [1997], Pascazio and Facchi [1999], Kofman and Kurizki [1999, 2000], Facchi and Pascazio [2000], Facchi, Nakazato and Pascazio [2001]).

There are situations (e.g., oscillatory systems, whose Poincaré time is finite) where γ and $\mathcal{Z}$ cannot be defined. As we shall see, these cases require a different

treatment, for the very definition of Zeno effect becomes somewhat delicate. This will be discussed in §§ 6–8.

3.3. *Pitfalls: "repopulation" and conceptual difficulties*

The quantum Zeno effect has become very popular during the last decade, mainly because of an interesting idea due to Cook (Cook [1988]), who proposed to test the QZE with a two-level system, and the subsequent experiment performed by Itano and collaborators (Itano, Heinzen, Bollinger and Wineland [1990]). This experiment provoked a very lively debate and was discussed by many authors (Petrosky, Tasaki and Prigogine [1990, 1991], Peres and Ron [1990], Ballentine [1991], Itano, Heinzen, Bollinger and Wineland [1991], Frerichs and Schenzle [1992], Inagaki, Namiki and Tajiri [1992], Home and Whitaker [1992, 1993], Blanchard and Jadczyk [1993], Pascazio, Namiki, Badurek and Rauch [1993], Altenmuller and Schenzle [1994], Pascazio and Namiki [1994], Schulman, Ranfagni and Mugnai [1994], Berry [1995], Beige and Hegerfeldt [1996], Schulman [1997], Thun and Peřina [1998]). However, we shall follow here a different route: rather than analyzing Cook's proposal and the related experiment, we shall consider a physically equivalent situation that better suits our discussion and can be easily compared to the analysis of the following sections.

The central mathematical quantity considered by Misra and Sudarshan (Misra and Sudarshan [1977]) is "the probability $\mathcal{P}(0,T;\rho_0)$ that no decay is found *throughout the interval* $\Delta = [0,T]$ when the initial state of the system was known to be ρ_0." (Italics in the original. Some symbols have been changed.) In the notation of § 3.1, this reads

$$\mathcal{P}(0,T;\rho_0) \equiv \lim_{N\to\infty} P^{(N)}(T). \tag{3.18}$$

Notice that the above-mentioned "survival probability" is the probability of finding the system in its initial state ρ_0 at *every* measurement, during the interval Δ. This is a subtle point, as we shall see.

Consider a three-level (atomic) system, shined by an rf field of frequency Ω, that provokes Rabi oscillations between levels $|+\rangle$ and $|-\rangle$. The equations of motion (2.6)–(2.7), with initial condition (in this section we omit the symbol $^{\mathrm{T}}$ of vector Transposition) $\boldsymbol{R}(0) \equiv (0,0,1)$ (only level $|+\rangle$ is initially populated), yield

$$\boldsymbol{R}(t) = (0, \sin 2\Omega t, \cos 2\Omega t). \tag{3.19}$$

If the transition between the two levels is driven by an on-resonant $\pi/2$ pulse, of duration

$$T = \frac{\pi}{2\Omega}, \tag{3.20}$$

one gets $\boldsymbol{R}(T) \equiv (0,0,-1)$, so that only level $|-\rangle$ is populated at time T.

Perform a measurement at time $\tau = T/N = \pi/2N\Omega$, by shining on the system a very short "measurement" pulse, that provokes transitions from level $|-\rangle$ to a third level $|M\rangle$, followed by the rapid spontaneous emission of a photon. The measurement pulse "projects" the atom onto level $|-\rangle$ or $|+\rangle$ and "kills" the off-diagonal terms $\rho_{\pm\mp}$ of the density matrix, while leaving unaltered its diagonal terms $\rho_{\pm\pm}$, so that, from eq. (2.10),

$$\boldsymbol{R}\left(\frac{\pi}{2N\Omega}\right) = \left(0, \sin\frac{\pi}{N}, \cos\frac{\pi}{N}\right) \overset{\text{measurement}}{\longrightarrow} \left(0,0,\cos\frac{\pi}{N}\right) \equiv \boldsymbol{R}^{(1)}. \tag{3.21}$$

Then the evolution restarts, always governed by eq. (2.6), but with the new initial condition $\boldsymbol{R}^{(1)}$. After N measurements, at time $T = N\tau = \pi/2\Omega$,

$$\boldsymbol{R}(T) = \left(0,0,\cos^N\frac{\pi}{N}\right) \equiv \boldsymbol{R}^{(N)} \tag{3.22}$$

and the probabilities that the atom is in level $|+\rangle$ or $|-\rangle$ read (see eq. 2.9)

$$\mathcal{P}_+^{(N)}(T) = \tfrac{1}{2}\left(1 + R_3^{(N)}\right) = \tfrac{1}{2}\left(1 + \cos^N\frac{\pi}{N}\right), \tag{3.23}$$

$$\mathcal{P}_-^{(N)}(T) = \tfrac{1}{2}\left(1 - R_3^{(N)}\right) = \tfrac{1}{2}\left(1 - \cos^N\frac{\pi}{N}\right), \tag{3.24}$$

respectively. Since $\mathcal{P}_+^{(N)}(T) \to 1$ and $\mathcal{P}_-^{(N)}(T) \to 0$ as $N \to \infty$, this looks like a quantum Zeno effect. However, it is *not* the quantum Zeno effect à la Misra and Sudarshan: eq. (3.23) [(3.24)] expresses only the probability that the atom is in level $|+\rangle$ [$|-\rangle$] at time T, after N measurements, *independently* of its past history. In particular, eqs. (3.23)–(3.24) take into account the *possibility that one level gets repopulated after the atom has made transitions to the other level*. In order to shed light on this rather subtle point, let us look explicitly at the first two measurements.

After the first measurement, by eq. (3.21),

$$R_3^{(1)} = \cos\frac{\pi}{N} = \cos^2\frac{\pi}{2N} - \sin^2\frac{\pi}{2N} = \mathcal{P}_+^{(1)} - \mathcal{P}_-^{(1)}, \tag{3.25}$$

where $\mathcal{P}_{\pm}^{(1)}$ is the occupation probability of level $|\pm\rangle$ at time $\tau = \pi/2N\Omega$, after the first measurement pulse. After the second measurement, one obtains

$$R_3^{(2)} = \cos^2 \frac{\pi}{N} = \mathcal{P}_+^{(2)} - \mathcal{P}_-^{(2)}, \tag{3.26}$$

where the occupation probabilities at time $2\tau = \pi/N\Omega$ read

$$\mathcal{P}_+^{(2)} = \tfrac{1}{2}\left(1 + R_3^{(2)}\right) = \cos^4 \frac{\pi}{2N} + \sin^4 \frac{\pi}{2N}, \tag{3.27}$$

$$\mathcal{P}_-^{(2)} = \tfrac{1}{2}\left(1 - R_3^{(2)}\right) = 2\sin^2 \frac{\pi}{2N} \cos^2 \frac{\pi}{2N}. \tag{3.28}$$

It is then obvious that $\mathcal{P}_+^{(2)}$, in eq. (3.27), is *not the survival probability* of level $|+\rangle$, according to definition (3.18). It is just the probability that level $|+\rangle$ is populated at time $t = \pi/N\Omega$, including the possibility that the transition $|+\rangle \to |-\rangle \to |+\rangle$ took place, with probability $\sin^2(\pi/2N) \cdot \sin^2(\pi/2N) = \sin^4(\pi/2N)$. By contrast, the *survival* probability, namely the probability that the atom is found in level $|+\rangle$ *both* at the first and second measurements, is given by $\mathcal{P}_+^{(1,2)} = \cos^2(\pi/2N) \cdot \cos^2(\pi/2N) = \cos^4(\pi/2N)$. Figure 7 shows what happens during the first two measurements.

After N measurements, the probability that level $|+\rangle$ is populated at time T, independently of its "history", is given by eq. (3.23), and includes the possibility that transitions to level $|-\rangle$ took place. As a matter of fact, it is not difficult to realize that eqs. (3.23)–(3.24) conceal a binomial distribution:

$$\begin{aligned}
\sum_{n\ \text{even}} \binom{N}{n} s^{2n} c^{2(N-n)} &= c^{2N} \sum_{n\ \text{even}} \binom{N}{n} (s/c)^{2n} \\
&= \frac{c^{2N}}{2} \sum_{n=0}^{N} \left[\binom{N}{n} \left(\frac{s}{c}\right)^{2n} + \binom{N}{n} (-1)^n \left(\frac{s}{c}\right)^{2n} \right] \\
&= \frac{c^{2N}}{2} \left[(1 + (s/c)^2)^N + (1 - (s/c)^2)^N \right] \\
&= \tfrac{1}{2}\left[1 + \cos^N(\pi/N)\right] \\
&= \mathcal{P}_+^{(N)}(T),
\end{aligned} \tag{3.29}$$

where $\sum_{n\ \text{even}}$ is a sum over all even values of n between 0 and N, $s = \sin(\pi/2N)$ and $c = \cos(\pi/2N)$. Clearly, eq. (3.23) includes all possible transitions between levels $|+\rangle$ and $|-\rangle$ and is conceptually very different from Misra and Sudarshan's

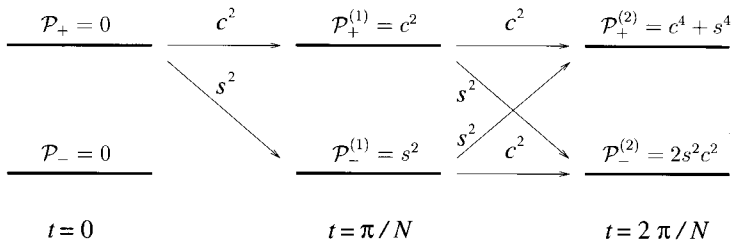

Fig. 7. Transition probabilities after the first two measurements for an oscillating system [$s = \sin(\pi/2N)$ and $c = \cos(\pi/2N)$].

survival probability (3.18). The correct formula for the survival probability, in the present case, is obtained by considering *only* the $n = 0$ term in eq. (3.29):

$$P_+^{(N)}(T) = \cos^{2N} \frac{\pi}{2N}. \tag{3.30}$$

This is a *bona fide* "survival probability", namely the probability that level $|+\rangle$ is populated at every measurement, at times $n\tau = nT/N$ ($n = 1, \ldots, N$).

The conclusions drawn in this section are always valid when the temporal behavior of the system under investigation is of the oscillatory type and no precautions are taken in order to prevent repopulation of the initial state (Nakazato, Namiki, Pascazio and Rauch [1996]). For instance, this problematic feature is present in the interesting proposal by Cook [1988] and the beautiful experiment by Itano, Heinzen, Bollinger and Wineland [1990]. On the other hand, no repopulation of the initial state takes place in other experiments involving neutron spin (Pascazio, Namiki, Badurek and Rauch [1993]) or photon polarization (Kwiat, Weinfurter, Herzog, Zeilinger and Kasevich [1995]).

We have seen that $P_+^{(N)}(T)$, in eq. (3.30), is a *bona fide* survival probability, but $\mathcal{P}_+^{(N)}(T)$, in eq. (3.23) is not (at least not according to Misra and Sudarshan's definition). However, both quantities tend to the same limiting value 1 as $N \to \infty$ and for large N the evolution is, in fact, hindered. We are therefore led to wonder whether it would not be meaningful to extend the notion of QZE beyond Misra and Sudarshan's definition of survival probability. This will be the subject of § 6.

§ 4. Dynamical quantum Zeno effect

In the usual formulation of QZE the measurement process is schematized by making use of projection operators à la von Neumann (Copenhagen

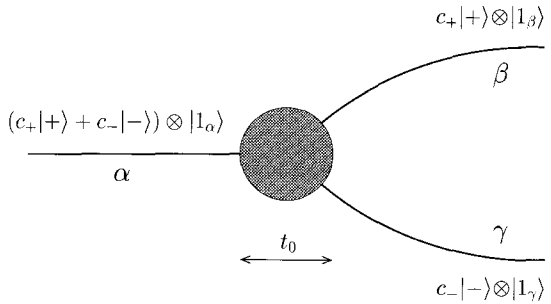

Fig. 8. The generalized spectral decomposition.

interpretation), without endeavoring to shed light on the underlying dynamics. However, a quantum-mechanical measurement is a very complicated physical process, taking place in a finite time and involving complex (macroscopic) physical systems.

It is possible to give a dynamical explanation of the Zeno effect (Pascazio and Namiki [1994], Pascazio [1997]), that involves only the Schrödinger equation and makes no use of projection operators. Let us briefly sketch how this is accomplished by introducing the notion of "generalized spectral decomposition" (GSD).

Consider again a two level system, prepared in a superposed state. A GSD is a dynamical (Hamiltonian) process by which different states of the system become associated (entangled) with different external "channels" (e.g., different degrees of freedom of a larger system). See fig. 8. One can think, for example, of a two-level atomic system getting entangled with different photon states of the electromagnetic field. The notion of "spectral decomposition" was introduced by Wigner [1963], who considered the Stern-Gerlach decomposition of an initial spin state, where each component of the spin becomes associated with a different wave packet. It is worth observing that the external channels the system gets entangled with need not be "external": for example, different wave packets of the system itself can act as "external" degrees of freedom.

A GSD is realized by the following Hamiltonian:

$$H_{\mathrm{GSD}}(t) \equiv g(t)\left[|+\rangle\langle+|\sigma_\beta + |-\rangle\langle-|\sigma_\gamma\right]\sigma_\alpha \equiv g(t)H', \qquad \int_0^{t_0} g(t)\,\mathrm{d}t = \tfrac{1}{2}\pi, \tag{4.1}$$

where the interaction is switched on during the time interval $[0, t_0]$, g is a real

function, $\sigma_\mu^\dagger = \sigma_\mu$ (the index $\mu = \alpha, \beta, \gamma$ labels the channel in fig. 8) and the effect of σ_μ is defined by

$$\sigma_\mu|0_\mu\rangle = |1_\mu\rangle, \qquad \sigma_\mu|1_\mu\rangle = |0_\mu\rangle, \tag{4.2}$$

so that if there is a "particle" in channel μ the operator σ_μ destroys it, while if there is no particle, σ_μ creates one. The effect of σ_μ $(\forall\mu)$ is therefore identical to that of the first Pauli matrix. We set

$$\left[\sigma_\mu, \sigma_\nu\right] = 0. \tag{4.3}$$

The action of the Hamiltonian H_{GSD} is

$$H_{\mathrm{GSD}}\,(c_+|+\rangle + c_-|-\rangle)\otimes|1_\alpha, 0_\beta, 0_\gamma\rangle \propto \left(c_+|+\rangle\otimes|0_\alpha, 1_\beta, 0_\gamma\rangle + c_-|-\rangle\otimes|0_\alpha, 0_\beta, 1_\gamma\rangle\right) \tag{4.4}$$

and consists in sending the $|+\rangle$ ($|-\rangle$) state of the system in the upper (lower) channel in fig. 8, thus performing a GSD.

In general, the only effect of a GSD is to set up a perfect correlation between the two states of the system and different external channels (namely, a univocal and unambiguous correspondence between different states of the system and different external channels). This is easily accomplished: the evolution engendered by H_{GSD} can be explicitly calculated (Pascazio and Namiki [1994]) and the result is

$$\begin{aligned}&\exp\left[-\mathrm{i}\int_0^{t_0} H_{\mathrm{GSD}}(t')\,\mathrm{d}t'\right](c_+|+\rangle + c_-|-\rangle)\otimes|1_\alpha\rangle \\ &\quad = -\mathrm{i}\left(c_+|+\rangle\otimes|1_\beta\rangle + c_-|-\rangle\otimes|1_\gamma\rangle\right) \quad (t > t_0),\end{aligned} \tag{4.5}$$

where we suppressed all 0s for simplicity.

A projection operator represents an *instantaneous* measurement. This is clearly a very idealized situation that cannot correspond to a real physical process, taking place at a microscopic level. The problem is therefore to understand how we can simulate such an instantaneous and unphysical process in our analysis, that makes use *only* of unitary evolutions. We observe that, in general, a GSD must take place in a very short time. Obviously, the term "very short time" must be understood at a macroscopic level of description, because the time microscopically required to efficaciously perform a GSD can be very long. Therefore, if we restrict our analysis to a macroscopic level of description, we can describe an (almost) instantaneous GSD by means of the so-called impulse approximation

$$\int_0^{t_0} g(t)\,\mathrm{d}t = \tfrac{1}{2}\pi, \quad t_0 \to 0^+, \tag{4.6}$$

which roughly amounts to setting $g(t) \to \frac{1}{2}\pi\delta(t)$ as $t_0 \to 0$, where δ is the Dirac function $\int_0^{t_0}\delta(t) = 1$. This is our alternative description of a von Neumann-like

instantaneous projection. It is a good approximation of the physical situation whenever t_0 is much shorter than the characteristic time of the free evolution of the system under observation.

By making repeated use of GSDs it is very simple to get quantum Zeno dynamics. A general proof is given by Pascazio and Namiki [1994] (a somewhat simpler version can be found in Pascazio [1997]), but here let us only sketch the main idea by looking at the example (2.1). The initial state (2.3), that we rewrite by including the external channel (wave packet) in the description,

$$|\Psi_0\rangle = |+\rangle \otimes |1_\alpha\rangle, \tag{4.7}$$

evolves after a short time τ into state (2.4):

$$|\Psi_\tau\rangle = \mathrm{e}^{-\mathrm{i}H_\mathrm{I}\tau}|\Psi_0\rangle = \left[\cos(\Omega\tau)|+\rangle - \mathrm{i}\sin(\Omega\tau)|-\rangle\right] \otimes |1_\alpha\rangle. \tag{4.8}$$

The GSD then yields (for $t_0 \ll \Omega^{-1}$)

$$\begin{aligned} |\Psi_{\tau+t_0}\rangle &= \exp\left[-\mathrm{i}\int_0^{t_0} H_\mathrm{GSD}(t')\,\mathrm{d}t'\right]|\Psi_\tau\rangle \\ &\propto \cos(\Omega\tau)|+\rangle \otimes |1_\beta\rangle - \mathrm{i}\sin(\Omega\tau)|-\rangle \otimes |1_\gamma\rangle, \end{aligned} \tag{4.9}$$

apart from a phase factor. Observe that the quantum coherence is perfectly preserved, during this evolution. At the next "step" of the evolution, channels β and γ become new incoming channels and the system evolves again under the action of H_I for a time τ and H_GSD for a time t_0. After N steps the final wave function reads

$$\begin{aligned} |\Psi_{N(\tau+t_0)}\rangle &= \prod_{n=1}^{N}\left\{\exp\left[-\mathrm{i}\int_0^{t_0} H_\mathrm{GSD}^{(n)}(t')\,\mathrm{d}t'\right]\exp[-\mathrm{i}H_\mathrm{I}\tau]\right\}|\Psi_0\rangle \\ &\propto \cos^N(\Omega\tau)|+\rangle \otimes |1_\beta^{(N)}\rangle + \mathrm{O}(N^{-1}), \end{aligned} \tag{4.10}$$

where $H_\mathrm{GSD}^{(n)}$ is the Hamiltonian that performs a generalized spectral decomposition at the nth step and $|1_\beta^{(N)}\rangle$ (all 0s were suppressed) represent the wave packet traveling in channel β at step N. Note that $N(\tau + t_0)$ is kept finite.

The contribution of all the other channels is $\mathrm{O}(N^{-1})$: a QZE is obtained because the particle, initially in state (4.7), ends up with probability

$$[1 - \mathrm{O}(1/N^2)]^N \sim 1 - \mathrm{O}(1/N) \tag{4.11}$$

in state $|+\rangle \otimes |1_\beta^{(N)}\rangle$. The "external" degrees of freedom are irrelevant and can be traced out (or recombined with the initial one).

We would like to emphasize that the very dynamical mechanism leading to QZE is curious: QZE is obtained via repeated use of generalized spectral decompositions H_GSD's, even though the interaction Hamiltonian H_I "attempts" to drive $|+\rangle$ into $|-\rangle$ for a finite time $N\tau$. This is probably the reason why QZE is often considered a counterintuitive phenomenon.

§ 5. Continuous observation

A projection à la von Neumann (von Neumann [1932]) is a handy way to "summarize" the complicated physical processes that take place during a quantum measurement. A measurement process is performed by an external (macroscopic) apparatus and involves dissipative effects, that imply an exchange of energy with and often a flow of probability towards the environment. The external system performing the observation need not be a *bona fide* detection system, namely a system that "clicks" or is endowed with a pointer. It is enough that the information on the state of the observed system be encoded in the state of the apparatus. For instance, a spontaneous emission process is often a very effective measurement process, for it is irreversible and leads to an entanglement of the state of the system (the emitting atom or molecule) with the state of the apparatus (the electromagnetic field). The von Neumann rules arise when one traces away the photonic state and is left with an incoherent superposition of atomic states.

We shall now introduce several alternative descriptions of a measurement process and discuss the notion of continuous measurement. This is to be contrasted with the idea of pulsed measurements, discussed in § 3. Both formulations lead to QZE.

5.1. *Mimicking the projection with a non-Hermitian Hamiltonian*

It is useful for our discussion on the QZE and probably interesting on general grounds to see how the action of an external apparatus can be mimicked by a non-Hermitian Hamiltonian. Let us consider the following Hamiltonian:

$$H_\mathrm{I} = \begin{pmatrix} 0 & \Omega \\ \Omega & -\mathrm{i}2V \end{pmatrix} = -\mathrm{i}V\mathbf{1} + \boldsymbol{h}\cdot\boldsymbol{\sigma}, \quad \boldsymbol{h} = (\Omega, 0, \mathrm{i}V)^\mathrm{T}, \tag{5.1}$$

that yields Rabi oscillations of frequency Ω, but at the same time absorbs away the $|-\rangle$ component of the Hilbert space, performing in this way a "measurement".

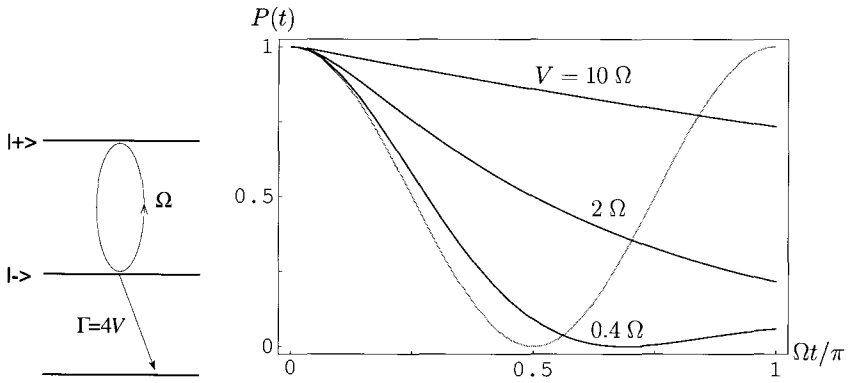

Fig. 9. Survival probability for a system undergoing Rabi oscillations in the presence of absorption ($V = 0.4, 2, 10\Omega$). The gray line is the undisturbed evolution ($V = 0$).

Due to the non-Hermitian features of this description, probabilities are not conserved: we are concentrating our attention only on the $|+\rangle$ component.

An elementary SU(2) manipulation yields the following evolution operator:

$$e^{-iH_1 t} = e^{-Vt}\left[\cosh(ht) - i\frac{\boldsymbol{h}\cdot\boldsymbol{\sigma}}{h}\sinh(ht)\right], \tag{5.2}$$

where $h = \sqrt{V^2 - \Omega^2}$ and we supposed $V > \Omega$. Let the system be initially prepared in the state (2.3): the survival amplitude reads

$$\begin{aligned}\mathcal{A}(t) &= \langle\psi_0|e^{-iH_1 t}|\psi_0\rangle \\ &= e^{-Vt}\left[\cosh(\sqrt{V^2-\Omega^2}t) + \frac{V}{\sqrt{V^2-\Omega^2}}\sinh(\sqrt{V^2-\Omega^2}t)\right] \\ &= \tfrac{1}{2}\left(1 + \frac{V}{\sqrt{V^2-\Omega^2}}\right)e^{-(V-\sqrt{V^2-\Omega^2})t} \\ &\quad + \tfrac{1}{2}\left(1 - \frac{V}{\sqrt{V^2-\Omega^2}}\right)e^{-(V+\sqrt{V^2-\Omega^2})t}.\end{aligned} \tag{5.3}$$

The above results are exact and display some interesting and very general aspects of the quantum Zeno dynamics. The survival probability $P(t) = |\mathcal{A}(t)|^2$ is shown in fig. 9 for $V = 0.4, 2, 10\Omega$. As expected, probability is (exponentially) absorbed away as $t \to \infty$. However, as V increases, by using eq. (5.3), the survival probability reads

$$P(t) \sim \left(1 + \frac{\Omega^2}{2V}\right)\exp\left(-\frac{\Omega^2}{V}t\right), \tag{5.4}$$

and the effective decay rate $\gamma_{\text{eff}}(V) = \Omega^2/V$ becomes smaller, eventually halting the "decay" (absorption) of the initial state and yielding an interesting example

of QZE: a larger V entails a more "effective" measurement of the initial state. We emphasize that the expansion (5.4) becomes valid very quickly, on a time scale of order V^{-1}. Notice that this example is not affected by the repopulation drawback described in § 3.3 (once the probability is absorbed away, it does not flow back to the initial state).

5.2. *Coupling with a flat continuum*

We now show that the non-Hermitian Hamiltonian (5.1) can be obtained by considering the evolution engendered by a Hermitian Hamiltonian acting on a larger Hilbert space and then restricting the attention to the subspace spanned by $\{|+\rangle, |-\rangle\}$. Consider the Hamiltonian

$$H = \Omega(|+\rangle\langle -| + |-\rangle\langle +|) + \int d\omega\, \omega|\omega\rangle\langle\omega| + \sqrt{\frac{\Gamma}{2\pi}}\int d\omega\, (|-\rangle\langle\omega| + |\omega\rangle\langle -|), \tag{5.5}$$

which describes a two-level system coupled to the photon field in the rotating-wave approximation. The state of the system at time t can be written as

$$|\psi_t\rangle = x(t)|+\rangle + y(t)|-\rangle + \int d\omega\, z(\omega, t)|\omega\rangle, \tag{5.6}$$

and the Schrödinger equation reads

$$\begin{aligned} i\dot{x}(t) &= \Omega y(t), \\ i\dot{y}(t) &= \Omega x(t) + \sqrt{\frac{\Gamma}{2\pi}}\int d\omega\, z(\omega, t), \\ i\dot{z}(\omega, t) &= \omega z(\omega, t) + \sqrt{\frac{\Gamma}{2\pi}}\, y(t). \end{aligned} \tag{5.7}$$

By using the initial condition $x(0) = 1$ and $y(0) = z(\omega, 0) = 0$ one obtains

$$z(\omega, t) = -i\sqrt{\frac{\Gamma}{2\pi}}\int_0^t d\tau\, e^{-i\omega(t-\tau)}y(\tau) \tag{5.8}$$

and

$$i\dot{y}(t) = \Omega x(t) - i\frac{\Gamma}{2\pi}\int d\omega \int_0^t d\tau\, e^{-i\omega(t-\tau)}y(\tau) = \Omega x(t) - i\frac{\Gamma}{2}y(t). \tag{5.9}$$

Therefore $z(\omega, t)$ disappears from the equations and we get two first-order differential equations for x and y. The only effect of the continuum is the

appearance of the imaginary frequency $-i\Gamma/2$. Incidentally, this is ascribable to the "flatness" of the continuum [there is no form factor or frequency cutoff in the last term of eq. (5.5)], which yields a purely exponential (Markovian) decay of $y(t)$.

In conclusion, the dynamic in the subspace spanned by $|+\rangle$ and $|-\rangle$ reads

$$i\dot{x}(t) = \Omega y(t), \qquad i\dot{y}(t) = -i\frac{\Gamma}{2}y + \Omega x(t). \tag{5.10}$$

Of course, this dynamic is not unitary, for probability flows out of the subspace, and is generated by the non-Hermitian Hamiltonian

$$H = \Omega(|+\rangle\langle -| + |-\rangle\langle +|) - i\frac{\Gamma}{2}|-\rangle\langle -|. \tag{5.11}$$

This Hamiltonian is the same as (5.1) when one sets $\Gamma = 4V$. QZE is obtained by increasing Γ: a larger coupling to the environment leads to a more effective "continuous" observation on the system (quicker response of the apparatus), and as a consequence to a slower decay (QZE).

The processes described in this section and the previous one can therefore be viewed as "continuous" measurements performed on the initial state. The non-Hermitian term $-2iV$ is proportional to the decay rate Γ of state $|-\rangle$, quantitatively $\Gamma = 4V$. Therefore, state $|-\rangle$ is continuously monitored with a response time $1/\Gamma$: as soon as it becomes populated, it is detected within a time $1/\Gamma$. The "strength" $\Gamma = 4V$ of the observation can be compared to the frequency $\tau^{-1} = (t/N)^{-1}$ of measurements in the "pulsed" formulation. Indeed, for large values of Γ one gets from eq. (5.4)

$$\gamma_{\text{eff}}(\Gamma) \sim \frac{4\Omega^2}{\Gamma} = \frac{4}{\tau_Z^2\Gamma}, \quad \text{for} \quad \Gamma \to \infty, \tag{5.12}$$

which, compared with eq. (3.13), yields an interesting relation between continuous and pulsed measurements (Schulman [1998])

$$\Gamma \simeq \frac{4}{\tau} = \frac{4N}{t}. \tag{5.13}$$

5.3. *Continuous Rabi observation*

The two previous examples might lead the reader to think that absorption and/or probability leakage to the environment (or in general to other degrees

of freedom) are fundamental requisites to obtain QZE. This expectation would be incorrect. Let us analyze a somewhat different situation by coupling one of the two levels of the system to a third one, which will play the role of a measuring apparatus. The (Hermitian) Hamiltonian is

$$H_I = \Omega(|+\rangle\langle -| + |-\rangle\langle +|) + K(|-\rangle\langle M| + |M\rangle\langle -|) = \begin{pmatrix} 0 & \Omega & 0 \\ \Omega & 0 & K \\ 0 & K & 0 \end{pmatrix}, \tag{5.14}$$

where $K \in \mathbb{R}$ is the strength of the coupling to the new level M, and

$$\langle +| = (1,0,0), \quad \langle -| = (0,1,0), \quad \langle M| = (0,0,1). \tag{5.15}$$

This is probably the simplest way to include an "external" apparatus in our description: as soon as the system is in $|-\rangle$, it undergoes Rabi oscillations to $|M\rangle$. Similar examples were considered by Peres [1980] and Kraus [1981]. We expect level $|M\rangle$ to perform better as a measuring apparatus when the strength K of the coupling becomes larger.

The above Hamiltonian is easily diagonalized. Its eigenvalues and eigenvectors are

$$\lambda_0 = 0, \qquad |u_0\rangle = \frac{1}{\sqrt{K^2+\Omega^2}}\begin{pmatrix} K \\ 0 \\ -\Omega \end{pmatrix},$$
$$\lambda_\pm = \pm\sqrt{K^2+\Omega^2}, \qquad |u_\pm\rangle = \frac{1}{\sqrt{2(K^2+\Omega^2)}}\begin{pmatrix} \pm\sqrt{K^2+\Omega^2} \\ \Omega \\ K \end{pmatrix}. \tag{5.16}$$

Let the initial state be

$$|\psi_0\rangle = |+\rangle = \frac{1}{\sqrt{K^2+\Omega^2}}\left(K|u_0\rangle + \frac{\Omega}{\sqrt{2}}|u_-\rangle + \frac{\Omega}{\sqrt{2}}|u_-\rangle\right). \tag{5.17}$$

The evolution is easily computed:

$$|\psi_t\rangle = e^{-iH_It}|\psi_0\rangle = \frac{1}{\sqrt{K^2+\Omega^2}}\left(K|u_0\rangle + \frac{\Omega}{\sqrt{2}}e^{-i\lambda_+t}|u_-\rangle + \frac{\Omega}{\sqrt{2}}e^{-i\lambda_-t}|u_-\rangle\right) \tag{5.18}$$

and the survival probability reads

$$P(t) = \frac{1}{(K^2+\Omega^2)^2}\left[K^2 + \Omega^2\cos(\sqrt{K^2+\Omega^2}\,t)\right]^2. \tag{5.19}$$

This is shown in fig. 10 for $K = 1, 3, 9\Omega$.

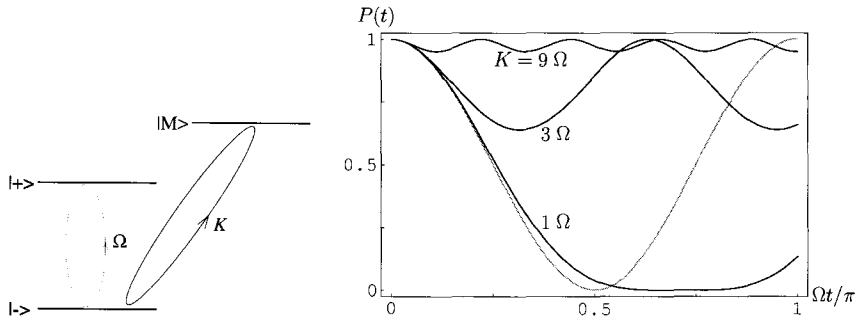

Fig. 10. Survival probability for a continuous Rabi "measurement" with $K = 1, 3, 9\Omega$: quantum Zeno effect.

We notice that for large K the state of the system does not change much: as K is increased, level $|M\rangle$ performs a better "observation" of the state of the system, hindering transitions from $|+\rangle$ to $|-\rangle$. This can be viewed as a QZE due to a "continuous", yet Hermitian observation performed by level $|M\rangle$.

This simple example triggers also another remarkable observation. The Zeno time is easily computed and turns out to be much longer than the Poincaré time (we are assuming $K \gg \Omega$)

$$\tau_Z = \Omega^{-1} \gg T_P = O(K^{-1}). \tag{5.20}$$

As a matter of fact, the Zeno time yields only the convexity of the survival probability in the origin: it does not give any relevant information about the duration of the short-time quadratic region. This contradicts many erroneous claims in the literature of the last few years. We shall come back to this point in § 8.

A few more comments are necessary. First of all, the example considered in this section is not free from repopulation effects like those considered in § 3.3. As a matter of fact, the situation here is even worse: unlike the case studied in § 3.3, where there was a probability repopulation of the initial state, in the present case there is a (coherent) amplitude repopulation phenomenon. However, even if these cases are at variance with Misra and Sudarshan's definition [see (3.18) and the paragraph preceding it], they call, in our opinion, for a broader formulation of QZE. This will be proposed in the following section.

Let us see how "effective" the Rabi "measurement" is, compared to the case of pulsed measurements. Notice that by performing pulsed observations on system (2.1) one gets from eq. (3.5)

$$P^{(N)}(t) = P\left(\frac{t}{N}\right)^N = \left(\cos\frac{\Omega t}{N}\right)^{2N} \sim \left(1 - \frac{\Omega^2 t^2}{N^2}\right)^N \sim 1 - \frac{\Omega^2 t^2}{N}, \tag{5.21}$$

for large values of N. On the other hand, in the present case of continuous observation, for large values of K, eq. (5.19) reads

$$\begin{aligned} P^{(K)}(t) &\sim \left(1 - 2\frac{\Omega^2}{K^2}\right)\left(1 + 2\frac{\Omega^2}{K^2}\cos(\sqrt{K^2 + \Omega^2}\, t)\right) \\ &\sim 1 - 4\frac{\Omega^2}{K^2}\sin^2\left(\frac{\sqrt{K^2 + \Omega^2}}{2}t\right) \end{aligned} \tag{5.22}$$

whence, by taking the average over a very short time of order $1/K$,

$$\overline{P^{(K)}(t)} \sim 1 - 2\frac{\Omega^2}{K^2}. \tag{5.23}$$

By comparing eq. (5.21) and eq. (5.23), one sees that the evolution is hindered (QZE) for

$$\frac{\Omega^2 t^2}{N} \simeq \frac{2\Omega^2}{K^2} \ (\ll 1), \tag{5.24}$$

namely

$$K \simeq \frac{\sqrt{2N}}{t}. \tag{5.25}$$

This relation is similar to (5.13): strong coupling is equivalent to frequent measurements.

A final comment is in order. All the situations analyzed in § 5 lead to QZE but never to IZE. The reason for this is profound and lies in the absence of the form factors of the interactions. The importance of form factors and the role they play in this context will be discussed later.

§ 6. Novel definition of quantum Zeno effect

The diverse examples and particular cases considered in the previous sections motivate us to look for a broader definition of Zeno effect, that includes "continuous" observations as well as somewhat delicate situations in which repopulation effects (in amplitude or probability) take place.

Let us consider a quantum system whose evolution is described by a Hamiltonian H. Let the initial state be ρ_0 (not necessarily a pure state) and the

survival probability $P(t)$. Consider the evolution of the system under the effect of an additional interaction, so that the total Hamiltonian reads

$$H_K = H + H_{\text{meas}}(K), \tag{6.1}$$

where K is a set of parameters and $H_{\text{meas}}(K = 0) = 0$. This Hamiltonian includes also as a particular case the GSD described in § 4; moreover, since a GSD is basically equivalent to a *bona fide* measurement, the above Hamiltonian includes, for all practical purposes, the usual formulation of quantum Zeno effect in terms of projection operators. Notice that H is not necessarily the free Hamiltonian; rather, one should think of H as a full Hamiltonian, containing interaction terms, and $H_{\text{meas}}(K)$ should be viewed as an "additional" interaction Hamiltonian performing the "measurement". We have considered many examples in this chapter: all of them fit in the scheme (6.1).

We shall say that the system displays a QZE if there exists an interval $I^{(K)} = [t_1^{(K)}, t_2^{(K)}]$ such that

$$P^{(K)}(t) > P(t), \qquad \forall t \in I^{(K)}, \tag{6.2}$$

where $P^{(K)}(t)$ and $P(t)$ are the survival probabilities under the action of the Hamiltonians H_K and H, respectively. We shall say that the system displays an *inverse* QZE if there exists an interval $I^{(K)}$ such that

$$P^{(K)}(t) < P(t), \qquad \forall t \in I^{(K)}. \tag{6.3}$$

The time interval $I^{(K)}$ must be evaluated case by case. However,

$$t_2^{(K)} \leqslant T_{\text{P}}, \tag{6.4}$$

where T_{P} is the Poincaré time. Obviously, for the definition (6.2)–(6.3) to be meaningful from a physical point of view, the length of the interval $I^{(K)}$ must be of order T_{P}. The above one is a very broad definition, for it includes a huge class of systems (even trivial cases like time translations $P(t) \to P(t - t_0)$ are included). We have not succeeded in finding a more restrictive definition and we do not think it would be meaningful. This is in line with our general philosophy: the Zeno effects are very common phenomena.

In order to elucidate the meaning of the above definition, let us look at some particular cases considered in this chapter. The situations considered in figs. 9 and 10 are both QZEs; according to this definition one has $t_1^{(K)} = 0$ and $t_2^{(K)} \leqslant T_{\text{P}} = \pi/\Omega$ [and $(t_2^{(K)} - t_1^{(K)}) = \text{O}(T_{\text{P}})$]. The case outlined in fig. 3 is also a QZE, with $t_1^{(K)} = 0$ and $t_2^{(K)} \leqslant T_{\text{P}}$ (notice that T_{P} may even be infinite).

If we deal with an unstable system, the definition of Zeno effect can be made more stringent, by simply generalizing the results of § 3.2 to a broader class of measurements. Indeed, in such a case, one need not refer to an interval $I^{(K)}$ and can consider the *global* behavior of the survival probability. By introducing the lifetime γ, one can define the occurrence of a QZE or an IZE if

$$\gamma_{\text{eff}}(K) \lessgtr \gamma, \tag{6.5}$$

respectively, where $\gamma_{\text{eff}}(K)$ is the new (effective) lifetime under the action of H_K. Notice that this case is in agreement with the definitions (6.2)–(6.3). Moreover, $t_2^{(K)} \to \infty$ for IZE, while $t_2^{(K)} \leqslant t_{\text{pow}}$ for QZE, where t_{pow} is the time at which a transition from an exponential to a power law takes place. [Such a time is of order log (coupling constant), at least for renormalizable quantum field theories (Facchi and Pascazio [1999]).] The definition (6.5) includes all the cases considered in § 3.2. See for example fig. 5b. Notice that when a Zeno effect is obtained by repeated use of projection operators (at equal time intervals τ), one always gets an exponential behavior with a well defined $\gamma_{\text{eff}}(\tau)$ (see § 3.2). A problem arises with oscillating systems (or in general with systems whose Poincaré time is finite) because of the impossibility of defining the "natural" decay rate γ (see, for instance, fig. 9). From this perspective, we cannot help feeling that the very concept of QZE is somewhat less meaningful for purely oscillating systems, exhibiting no *bona fide* instability.

We shall adopt these new definitions of Zeno effects in the following. They are novel and have not been proposed before. They work in all the cases considered in this chapter and also comprise, in a more general framework, all the examples of Zeno effects considered in the literature. These definitions should be kept in mind while considering the examples proposed in the following sections.

§ 7. Zeno effects in down-conversion processes

The differences and analogies between pulsed and continuous observations analyzed in the previous sections will now be discussed by considering a quantum optical example. A down-conversion process in a nonlinear crystal can be thought of as the decay of a pump photon into a pair of signal and idler photons of lower frequency. If the pumping is sufficiently strong and there is phase matching, the energy of the spontaneously down-converted light monotonously increases and that of the pump beam monotonously decreases. In this sense, the down-conversion process may be looked at as the decay process of an unstable system.

Let us first discuss the case of "pulsed" observation. There are similar ideas in the literature (Pascazio, Namiki, Badurek and Rauch [1993], Kwiat, Weinfurter, Herzog, Zeilinger and Kasevich [1995], Facchi, Klein, Pascazio and Schulman [1999]), but here we shall discuss an interesting example first proposed by Luis and Peřina [1996]. A pump beam illuminates a nonlinear crystal that is transversely cut in N pieces, which are then carefully aligned so that the signal and pump photons leave a given slice that becomes the input signal and pump photons for the next slice of the crystal, while the idler photons are taken out at each step (see fig. 12 in the following). By increasing the number N of slices, the probability of emission of the down-converted pair decreases: this is QZE. However, if the phase matching condition is not fulfilled in the process of down-conversion (Luis and Sánchez-Soto [1998], Thun and Peřina [1998]), the observation may, on the contrary, *enhance* the emission for a properly chosen N: this is an IZE.

We shall see that such a behaviour occurs also when, instead of cutting the crystal into N pieces, the idler beam is coupled to an auxiliary mode (see fig. 13 in the following). The continuous interaction with the auxiliary mode is a sort of "steady gaze" at the system and performs a continuous observation.

The Zeno–inverse Zeno interplay that takes place in this model can be easily understood in the light of the techniques outlined in § 3.2 and will be the object study of this section.

7.1. *The system*

Consider a nonlinear crystal through which three modes, pump p, signal s and idler i, propagate in the same direction. The nonlinear waveguide is filled with a second-order nonlinear medium in which ultraviolet pump photons are down-converted into signal and idler photons of lower frequency.

We will assume that all modes are monochromatic and their frequencies fixed, e.g., by placing narrow interference filters in front of the detectors. Provided the amplitudes of the fields vary little during an optical period (SVEA approximation), the effective Hamiltonian reads ($\hbar = 1$)

$$H = \omega_p a_p^\dagger a_p + \omega_s a_s^\dagger a_s + \omega_i a_i^\dagger a_i + \Gamma \left[a_p a_s^\dagger a_i^\dagger \mathrm{e}^{\mathrm{i}\Delta t} + a_p^\dagger a_s a_i \mathrm{e}^{-\mathrm{i}\Delta t} \right], \tag{7.1}$$

where ω_α is the frequency of mode α, $\Delta = (\boldsymbol{k}_p - \boldsymbol{k}_s - \boldsymbol{k}_i)_z$ is the nonlinear phase mismatch and the propagation variable z has been replaced with the evolution parameter t. The nonlinear coupling constant Γ is proportional to the second order nonlinear susceptibility $\chi(2)$ (Hong and Mandel [1985]). We suppose that

the incident pump field is intense and that the pump mode a_p can be treated classically, as a field of complex amplitude $a_p = \xi \exp(-\mathrm{i}\omega_p t)$, where ξ and ω_p denote the complex amplitude and the frequency of the classical pump wave, respectively. In this approximation the Hamiltonian (7.1) has only two quantized field modes and reads

$$H = \omega_s a_s^\dagger a_s + \omega_i a_i^\dagger a_i + \Gamma \left[a_s^\dagger a_i^\dagger \mathrm{e}^{-\mathrm{i}(\omega_p - \Delta)t} + a_s a_i \mathrm{e}^{\mathrm{i}(\omega_p - \Delta)t} \right], \tag{7.2}$$

where the amplitude ξ has been absorbed in the coupling constant Γ (taken real for simplicity). Notice that the strong pump wave approximation will cease to be valid once appreciable depletion of the pump field occurs. Therefore the solution of eq. (7.2) properly describes the process of parametric down-conversion under the restriction $\langle n_{s,i}(t) \rangle \ll |\xi|^2$, where n is the number operator, i.e., for sufficiently strong pumping and sufficiently weak nonlinear interaction.

By introducing the slowly varying operators

$$a_s' = \mathrm{e}^{\mathrm{i}(\omega_s - \Delta/2)t} a_s, \qquad a_i' = \mathrm{e}^{\mathrm{i}(\omega_i - \Delta/2)t} a_i, \tag{7.3}$$

which obey the same commutation rules as the a's, the Heisenberg equations of motions take the form

$$\dot{a}_s' = -\mathrm{i}[a_s', H'], \qquad \dot{a}_i' = -\mathrm{i}[a_i', H'], \tag{7.4}$$

with the time-independent Hamiltonian

$$H' = \frac{\Delta}{2} a_s'^\dagger a_s' + \frac{\Delta}{2} a_i'^\dagger a_i' + \Gamma \left[a_s'^\dagger a_i'^\dagger + a_s' a_i' \right], \tag{7.5}$$

where the frequency matching condition $\omega_p = \omega_s + \omega_i$ was used.

The state of the field at time $t = 0$ is taken to be the vacuum for the signal and idler modes

$$|\psi_0\rangle = |0_s, 0_i\rangle. \tag{7.6}$$

Under the action of the Hamiltonian (7.5) this state is unstable and spontaneously decays, continuously generating photon pairs. For example, when $\Delta = 0$, the average number of signal and idler photons originating in the crystal of length t,

$$\langle a_s^\dagger(t) a_s(t) \rangle \equiv \langle \psi_0 | a_s^\dagger(t) a_s(t) | \psi_0 \rangle = \langle \psi_0 | a_i^\dagger(t) a_i(t) | \psi_0 \rangle = \sinh^2(\Gamma t), \tag{7.7}$$

is an exponentially increasing function of t. In eq. (7.7) and henceforth all (slowly varying) operators are written without primes to simplify the notation.

Our interest is focused on the survival amplitude of the vacuum state under the action of the Hamiltonian (7.5). It is somewhat more convenient to consider the evolution of the following linear combinations

$$a = \frac{a_i + a_s}{\sqrt{2}}, \qquad b = \frac{a_i - a_s}{\sqrt{2}}. \tag{7.8}$$

In terms of these two modes the Hamiltonian (7.5) reads

$$H = \frac{\Delta}{2} a^\dagger a + \frac{\Gamma}{2}\left[a^{\dagger 2} + a^2\right] + \frac{\Delta}{2} b^\dagger b - \frac{\Gamma}{2}\left[b^{\dagger 2} + b^2\right] \tag{7.9}$$

and the modes a and b are completely decoupled.

It is now straightforward to evaluate the time evolution of $|\psi_0\rangle$ by considering the properties of the generalized two-photon coherent states (Mandel and Wolf [1995]). Remember that by letting $U(\mu, \nu)$ be a unitary transformation that generates the pseudo-annihilation operator

$$A(\mu, \nu) = U(\mu, \nu)\, a\, U^\dagger(\mu, \nu) = \mu a + \nu a^\dagger, \quad \text{with} \quad |\mu|^2 - |\nu|^2 = 1, \tag{7.10}$$

for two complex numbers μ, ν, the generalized two-photon coherent state $|[\mu, \nu; \upsilon]\rangle$ is defined by operating $U(\mu, \nu)$ on the coherent state $|\upsilon\rangle$, i.e.,

$$|[\mu, \nu; \upsilon]\rangle = U(\mu, \nu)|\upsilon\rangle. \tag{7.11}$$

The scalar product between this state and a coherent state has the following form

$$\langle \upsilon|[\mu, \nu; w]\rangle = \frac{1}{\sqrt{\mu}} \exp\left[-\tfrac{1}{2}|\upsilon|^2 - \tfrac{1}{2}|w|^2 - \frac{1}{2}\frac{\nu}{\mu}\upsilon^{*2} + \frac{w}{\mu}\upsilon^* + \frac{1}{2}\frac{\nu^*}{\mu} w^2\right], \tag{7.12}$$

and the most general unitary transformation that has the property (7.10) is

$$U(\mu, \nu) = \exp[-\mathrm{i}(K a^\dagger a + k a^2 + k^* a^{\dagger 2})], \tag{7.13}$$

where K is real and k, a constant. The complex numbers μ and ν are related to the parameters K and k by the relation

$$\begin{cases} \mu = \cosh(\Delta k) + \mathrm{i}\frac{K}{\Delta k}\sinh(\Delta k), \\ \nu = \mathrm{i}\frac{2k}{\Delta k}\sinh(\Delta k), \end{cases} \quad \text{with} \quad \Delta k = \sqrt{4k^2 - K^2}, \tag{7.14}$$

where we considered, for simplicity, k real.

Let us look at the survival amplitude of the vacuum state under the action of the quadratic Hamiltonian (7.9), corresponding to a two-photon interaction with a classical pump for the two independent modes a and b. By using eq. (7.12) this reads

$$\begin{aligned} \mathcal{A}(t) &= \langle 0_a, 0_b|\mathrm{e}^{-\mathrm{i}Ht}|0_a, 0_b\rangle = \langle 0_a, 0_b|[\mu_a(t), \nu_a(t); 0_a], [\mu_b(t), \nu_b(t); 0_b]\rangle \\ &= \frac{1}{\sqrt{\mu_a(t)\mu_b(t)}}. \end{aligned} \tag{7.15}$$

In our case

$$\mu_a(t) = \mu_b(t) = \cosh(\Delta\Gamma t) + \mathrm{i}\frac{\Delta}{2\Delta\Gamma}\sinh(\Delta\Gamma t), \quad \text{with} \quad \Delta\Gamma = \sqrt{\Gamma^2 - \frac{\Delta^2}{4}}, \tag{7.16}$$

whence one gets the survival probability

$$P(t) = |\mathcal{A}(t)|^2 = \frac{1}{|\mu_a(t)|^2} = \left[\cosh^2(\Delta\Gamma t) + \frac{\Delta^2}{4\Delta\Gamma^2}\sinh^2(\Delta\Gamma t)\right]^{-1}. \tag{7.17}$$

We can now look at the features of this system.

At short times

$$P(t) \sim 1 - \Delta\Gamma^2 t^2 - \frac{\Delta^2}{4} t^2 = 1 - \Gamma^2 t^2, \tag{7.18}$$

so that the Zeno time reads

$$\tau_Z^{-2} = \langle H^2\rangle = \frac{\Gamma^2}{4}\langle 0_a, 0_b|(a^2 a^{\dagger 2} + b^2 b^{\dagger 2})|0_a, 0_b\rangle = \Gamma^2. \tag{7.19}$$

The long-time behavior depends on the value of $\Delta\Gamma^2$ in (7.16): if $\Delta < 2\Gamma$, at long times,

$$P(t) \sim \left[\frac{1}{4}\mathrm{e}^{2\Delta\Gamma t} + \frac{\Delta^2}{16\Delta\Gamma^2}\mathrm{e}^{2\Delta\Gamma t}\right]^{-1} = \frac{4\Delta\Gamma^2}{\Gamma^2}\mathrm{e}^{-2\Delta\Gamma t} \tag{7.20}$$

so that

$$P(t) \sim \mathcal{Z}\mathrm{e}^{-\gamma t}, \quad \text{where} \quad \gamma = \sqrt{4\Gamma^2 - \Delta^2} \quad \text{and} \quad \mathcal{Z} = \frac{4\Gamma^2 - \Delta^2}{\Gamma^2}. \tag{7.21}$$

This formula, as already emphasized in § 3.2 (see eq. 3.17), is an excellent approximation at long times and enables us to discuss the Zeno–inverse Zeno

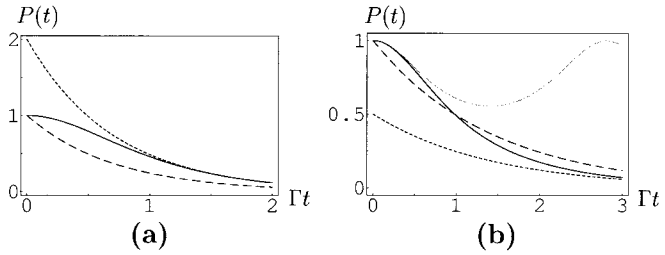

Fig. 11. Survival probability of the initial (vacuum) state. (a) $\Delta = \sqrt{2}\Gamma$ ($< \sqrt{3}\Gamma$) and $\mathcal{Z} = 2$; the solid line is the survival probability (7.17), the dotted line is the asymptotic exponential (7.21), and the dashed line is the renormalized exponential $\exp(-\gamma t)$. $P(t)$ and $\exp(-\gamma t)$ do not intersect, τ^* does not exist, and only a QZE is possible. (b) $\Delta = \sqrt{7/2}\Gamma$ ($\sqrt{3}\Gamma < \Delta < 2\Gamma$) and $\mathcal{Z} = 0.5$; the solid line is the survival probability (7.17), the dotted line is the asymptotic exponential (7.21), and the dashed line is the renormalized exponential $\exp(-\gamma t)$. $P(t)$ and $\exp(-\gamma t)$ intersect, τ^* exists, and a Zeno–inverse Zeno transition is possible. The gray line is the survival probability (7.22) for $\Delta = 3\Gamma$ ($> 2\Gamma$): in this case one gets an oscillatory behavior and $\mathcal{Z}$ cannot be defined.

transition. The condition $\mathcal{Z} < 1$ reads $\Delta > \sqrt{3}\Gamma$. In fig. 11 the vacuum survival probability (7.17) is shown for different values of the parameters. We shall see in § 8 that, in general, $\mathcal{Z}$ is due to the renormalization of the wave function.

As we have seen, when $\Delta < 2\Gamma$ the survival probability decreases exponentially; on the other hand, when $\Delta > 2\Gamma$ the behavior is oscillatory

$$P(t) = |\mathcal{A}(t)|^2 = \frac{1}{|\mu_a(t)|^2} = \left[\cos^2(|\Delta\Gamma|t) + \frac{\Delta^2}{4|\Delta\Gamma|^2}\sin^2(|\Delta\Gamma|t)\right]^{-1}, \quad (7.22)$$

with $4|\Delta\Gamma|^2/\Delta^2 < P(t) < 1$. In this case a decay rate γ and, as a consequence, $\mathcal{Z}$ cannot be defined. We note that the vacuum state never decays completely. We can now discuss pulsed and continuous observation.

7.2. *Pulsed observation*

Let us first consider pulsed observations performed at time intervals $\tau = t/N$ (Luis and Peřina [1996]). The nonlinear crystal is divided into N equal parts of length L/N, corresponding to an interaction time $\tau = t/N$, as shown in fig. 12. Assume that the signal beams at each slice are perfectly superimposed and aligned and that reflection at each step is made negligible, for instance by embedding the N pieces in a linear medium with exactly the same refractive index. On the other hand, the idler path is interrupted after each slice, for instance by means of mirrors. At each step the output idler beam is completely removed and replaced by a new input idler beam in the vacuum state. With this

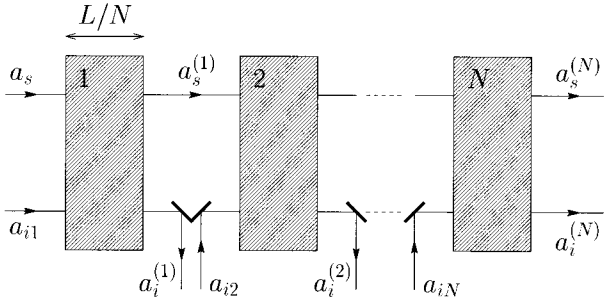

Fig. 12. Outline of a "sliced" parametric down-conversion scheme. The down-converter is cut into N crystals of length L/N. After each slice, the output idler beams $a_i^{(k)}$ are removed by means of mirrors inserted in the idler path and replaced by different input idler fields a_{ik} in vacuum.

modification it is possible to detect the emission of the idler photons, for instance, by means of N photodetectors.

By using the definition (7.8) and the evolution law (7.10) or, alternatively, by directly solving the Heisenberg equations (7.4) for the Hamiltonian (7.5), one gets for a single slice

$$\begin{cases} a_s(\tau) = \mu(\tau)a_s + \nu(\tau)a_i^\dagger \\ a_i(\tau) = \mu(\tau)a_i + \nu(\tau)a_s^\dagger \end{cases}, \quad (7.23)$$

where $\mu(t) = \mu_a(t)$ is defined by eq. (7.16) and $\nu(t) = \nu_a(t) = \mathrm{i}\Gamma\sinh(\Delta\Gamma t)/\Delta\Gamma$. Remember that unitarity requires $|\mu(t)|^2 - |\nu(t)|^2 = 1$.

We study how the survival probability of the vacuum state is modified by frequent interruptions of the idler path. To this end we will look at the modified evolution of the signal mode, following Luis and Peřina [1996], Luis and Sánchez-Soto [1998] and Thun and Peřina [1998]. By using (7.23) we can express the signal annihilation operator after the Nth slice $a_s^{(N)}$ in terms of the annihilation (creation) operator of the signal (idler) mode before it

$$a_s^{(N)} = \mu(\tau)a_s^{(N-1)} + \nu(\tau)a_{iN}^\dagger, \quad (7.24)$$

where we used the fact that a different vacuum mode a_{ik}, $k = 1, \ldots, N$, is at the idler input of each of the N crystals. By iterating eq. (7.24) we obtain

$$a_s^{(N)} = \mu^N a_s + \nu\sum_{k=1}^{N}\mu^{N-k}a_{ik}^\dagger. \quad (7.25)$$

The mean value of the number of signal photons reads

$$\langle a_s^{(N)\dagger}a_s^{(N)}\rangle = |\nu|^2\sum_{k=1}^{N}|\mu|^{2(N-k)} = |\nu|^2\frac{|\mu|^{2N}-1}{|\mu|^2-1} = |\mu|^{2N} - 1, \quad (7.26)$$

where the unitarity condition was used. For large values of N, by making use of eq. (7.17) we get

$$\langle a_s^{(N)\dagger} a_s^{(N)} \rangle = |\mu(t/N)|^{2N} - 1 = P(t/N)^{-N} - 1 \sim 1 - P(t/N)^N = 1 - P^{(N)}(t) \tag{7.27}$$

and the mean number of photons coincides with the probability of emitting one signal photon (for the probability of emission of more than one photon is negligible), i.e., with the (modified) decay probability of the vacuum state.

By using the short-times expansion of the survival probability (7.18) we get

$$P^{(N)}(t) \sim \exp(-\Gamma^2 \tau t), \tag{7.28}$$

i.e., an effective decay rate

$$\gamma_{\text{eff}}(\tau) = \Gamma^2 \tau, \tag{7.29}$$

which is in accord with eq. (3.13), because $\tau_Z = 1/\Gamma$ (as shown by eq. 7.19). In the $N \to \infty$ limit the effective decay rate approaches zero and the decay is completely frozen, i.e., no photons are emitted (QZE).

If, in (7.21),

$$\mathcal{Z} > 1 \Leftrightarrow \Delta < \sqrt{3}\Gamma, \tag{7.30}$$

we are in the situation outlined in figs. 6a and 11a, and according to the analysis of § 3.2 only a QZE can occur. On the other hand, if

$$\mathcal{Z} < 1, \tag{7.31}$$

then, according to the analysis of § 3.2 (see figs. 5 and 6), a transition time τ^* exists and by decreasing the frequency of measurements one observes the transition from a Zeno to an inverse Zeno (Heraclitus) regime. By using eq. (7.21), the condition (7.31) reads

$$\Delta > \sqrt{3}\Gamma. \tag{7.32}$$

In particular, if the phase mismatch Δ is close to the value $\Delta = 2\Gamma$, the linear approximation (7.29) is valid up to τ^*, because γ in eq. (7.21) approaches zero, and we get

$$\tau^* = \frac{t}{N^*} \simeq \frac{\gamma}{\Gamma^2} = \frac{\sqrt{4\Gamma^2 - \Delta^2}}{\Gamma^2} = \frac{2\Delta\Gamma}{\Gamma^2}, \tag{7.33}$$

whence for $N^* < \Gamma^2 t / 2\Delta\Gamma$ the photon production is enhanced (IZE).

So far, we supposed $\Delta < 2\Gamma$. The effect becomes more spectacular for $\Delta > 2\Gamma$ (see eq. 7.22). Indeed, in this case the phase mismatch is so large that the down-conversion process is no longer exponential, but has an oscillatory behavior

$$\begin{aligned} \langle a_s^\dagger(t) a_s(t) \rangle &= |\mu(t)|^2 - 1 = \cos^2(|\Delta\Gamma|t) + \frac{\Delta^2}{4|\Delta\Gamma|^2} \sin^2(|\Delta\Gamma|t) - 1 \\ &= \frac{\Gamma^2}{|\Delta\Gamma|^2} \sin^2(|\Delta\Gamma|t), \end{aligned} \tag{7.34}$$

which is bounded by

$$\langle a_s^\dagger(t) a_s(t) \rangle_{\text{MAX}} = \frac{\Gamma^2}{|\Delta\Gamma|^2}. \tag{7.35}$$

On the other hand, by cutting the crystal and removing the idler path, one gets

$$\langle a_s^{(N)\dagger} a_s^{(N)} \rangle = \left(1 + \frac{\Gamma^2 t^2}{N^2}\right)^N - 1 \sim \exp(\Gamma^2 \tau t) - 1, \tag{7.36}$$

and an explosive exponential behavior is recovered (IZE). It is easy to check that $\tau^* = 0$, a quite remarkable situation. Independently of the frequency of measurements N, one always obtains an IZE, see fig. 11b (a QZE is recovered only in the $N \to \infty$ limit). Remember also that $\mathcal{Z}$ cannot be defined, in this case. We will rigorously justify this interpretation in § 8, by considering complete and incomplete Rabi oscillations as the limiting case of a truly unstable system with a finite-width form factor.

We notice that the process described is always unitary and it actually makes no difference whether any measurements on the idler modes are actually carried out or not. It is sufficient that such measurements could *in principle* be made, as stressed in § 4. We also emphasize that the situation just analyzed is affected by (probability) repopulation effects like those described in § 3.3.

7.3. *The nonlinear coupler: continuous observation*

We now modify the system considered in the previous subsections and discuss continuous observation. Consider a nonlinear coupler made up of two waveguides, through which four modes, pump p, signal s, idler i and auxiliary mode b propagate in the same direction, see fig. 13. The nonlinear waveguide is again filled with a second-order nonlinear medium in which ultraviolet pump photons are down-converted to signal and idler photons of lower frequency,

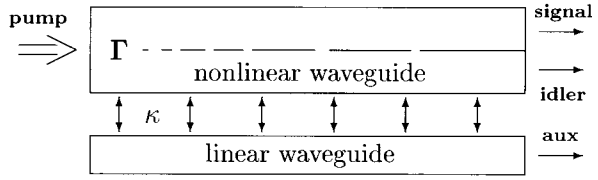

Fig. 13. Outline of the nonlinear coupler.

but in addition, the idler mode is allowed to exchange energy, e.g., by means of evanescent waves, with the auxiliary mode b propagating through a linear medium (Řeháček, Peřina, Facchi, Pascazio and Mišta [2000]).

We assume again the validity of the SVEA approximation and we consider the linear coupling weak enough so that it can be described by the coupled modes theory (Born approximation) (Stich and Bass [1985], Yariv and Yeh [1984], Saleh and Teich [1991]). With the help of the strong pump wave approximation the Hamiltonian of our problem is simplified as follows:

$$H_\kappa = H + H_{\mathrm{meas}}(\kappa), \quad \text{with} \quad H_{\mathrm{meas}}(\kappa) = \kappa(a_i^\dagger b + a_i b^\dagger) + \omega_b b^\dagger b, \tag{7.37}$$

where H is the down-converter Hamiltonian (7.2) and κ the linear coupling constant. By introducing the slowly varying operators (with a slightly different choice for a_s' and a_i', which is somewhat more convenient for the following discussion)

$$a_s' = \mathrm{e}^{\mathrm{i}\omega_s t} a_s, \qquad a_i' = \mathrm{e}^{\mathrm{i}(\omega_i - \Delta)t} a_i, \qquad b' = \mathrm{e}^{\mathrm{i}(\omega_b - \Delta)t} b, \tag{7.38}$$

we get, instead of (7.5), the new time-independent Hamiltonian

$$H_\kappa = \Delta a_i^\dagger a_i + \Gamma(a_s^\dagger a_i^\dagger + a_s a_i) + \Delta b^\dagger b + \kappa(a_i^\dagger b + a_i b^\dagger), \tag{7.39}$$

where we assumed again that the frequency matching conditions, $\omega_p - \omega_s - \omega_i = 0$ and $\omega_b = \omega_i$, hold and we suppressed all primes.

The dynamics of the nonlinear coupler (7.39) reduces to the dynamics of the spontaneous down-conversion process (7.5) provided that $\kappa = 0$. In the case of phase matching $\Delta = 0$, the average number of signal and idler photons originating in the crystal of length t, eq. (7.7), is an exponentially increasing function of t.

The behavior of the down-conversion process changes completely when one of the two down-converted modes (say, the idler mode) is coupled to an auxiliary

mode via the linear interaction, performing the "continuous observation". The Hamiltonian (7.39) yields, when $\Delta = 0$ (phase matching),

$$\begin{aligned} \dot{a}_s &= -\mathrm{i}\Gamma a_i^\dagger, \\ \dot{a}_i &= -\mathrm{i}\Gamma a_s^\dagger - \mathrm{i}\kappa b, \quad (\Delta = 0) \\ \dot{b} &= -\mathrm{i}\kappa a_i, \end{aligned} \tag{7.40}$$

and we are interested in the regime of weak nonlinearity, expressed by the condition $\kappa > \Gamma$. Notice that two opposite tendencies compete in eqs. (7.40): an elliptic structure, leading to oscillatory behavior, governed by the coupling parameter κ,

$$\ddot{a}_i = -\kappa^2 a_i, \qquad \ddot{b} = -\kappa^2 b \tag{7.41}$$

and a hyperbolic structure, yielding exponential behavior, governed by the nonlinear parameter Γ,

$$\ddot{a}_s = \Gamma^2 a_s, \qquad \ddot{a}_i = \Gamma^2 a_i. \tag{7.42}$$

The threshold between these two regimes occurs for $\Gamma \simeq \kappa$.

The system of equations (7.40) is easily solved and the number of output signal photons, which is the same as the number of pump photons decays, reads

$$\langle a_s^\dagger(t) a_s(t)\rangle = \frac{\Gamma^2}{\chi^2}\sin^2\chi t + \frac{\kappa^2\Gamma^2}{\chi^4}(1-\cos\chi t)^2, \tag{7.43}$$

where $\chi = \sqrt{\kappa^2 - \Gamma^2}$. Unlike the case of phase matched down-conversion (7.7), the exchange of energy between all modes now becomes periodical when $\kappa > \Gamma$. As the linear coupling becomes stronger, the period of the oscillations gets shorter and the amplitude of the oscillations decreases as κ^{-2}, namely

$$\langle a_s^\dagger(t) a_s(t)\rangle \sim \frac{\Gamma^2}{\kappa^2}\sin^2\kappa t + \frac{\Gamma^2}{\kappa^2}(1-\cos\kappa t)^2 = \frac{4\Gamma^2}{\kappa^2}\sin^2\frac{\kappa t}{2} \qquad (\kappa \gg \Gamma). \tag{7.44}$$

For strong coupling the down-conversion process is completely frozen, the medium becomes effectively linear and the pump photons propagate through it without "decay". [In the regime of very large κ, however, the coupled modes theory breaks down and some other experimental realization of the Hamiltonian (7.39) should be found.] Notice that in this situation, even if t is increased, the number of down-converted photons is bounded [compare with the opposite

case (7.7)]. This is QZE in the following sense: by increasing the coupling with the auxiliary mode, a better "observation" of the idler mode (and therefore of the decay of the pump) is performed and the evolution is hindered. There is an intuitive explanation of this behavior: since the linear coupling changes the phases of the amplitudes of the interacting modes, the constructive interference yielding exponential increase of the converted energy (7.7) is destroyed and down-conversion is frozen (see § 7.5 in the following).

In agreement with the final part of § 5.3, by comparing eq. (7.44) with eqs. (7.27)–(7.29), we find that the linear coupling is effective as the square root of the number of pulsed measurements, namely

$$\kappa = \frac{\sqrt{2N}}{t}. \tag{7.45}$$

Consider now the Hamiltonian (7.39) when $\kappa = 0$, describing down-conversion with phase mismatch Δ. It is apparent that the coupling and the phase mismatch influence the down-conversion process in the same way. Indeed for large values of the phase mismatch Δ it is easy to find from eq. (7.34) that

$$\langle a_s^\dagger(t) a_s(t)\rangle \sim \frac{4\Gamma^2}{\Delta^2}\sin^2\frac{\Delta t}{2} \qquad (\Delta \gg \Gamma), \tag{7.46}$$

which is to be compared with eq. (7.44). The interesting interplay between coupling κ and mismatch Δ will be investigated in the following subsection.

7.4. *Competition between the coupling and the mismatch*

In the previous section we saw that the nonlinear interaction was affected by both linear coupling and phase mismatch in the same way. The effectiveness of the nonlinear process drops down under their action. In this section we show that when both disturbing elements are present in the dynamics of the down-conversion process, the linear coupling can compensate for the phase mismatch and vice versa, so that the probability of emission of the signal and idler photons can almost return back to its undisturbed value.

We start from the equations of motion generated by the full interaction Hamiltonian (7.39)

$$\begin{cases} \dot a_s = -\mathrm{i}\Gamma a_i^\dagger, \\ \dot a_i = -\mathrm{i}\Delta a_i - \mathrm{i}\Gamma a_s^\dagger - \mathrm{i}\kappa b, \\ \dot b = -\mathrm{i}\Delta b - \mathrm{i}\kappa a_i \end{cases} \qquad (\Delta \neq 0, \kappa \neq 0). \tag{7.47}$$

Although it is easy to write down the explicit solution of the system (7.47), we shall provide only a qualitative discussion of the solution. The main features are

then best demonstrated with the help of a figure. Eliminating idler and auxiliary mode variables from eq. (7.47) we get a differential equation of the third order for the annihilation operator of the signal mode. Its characteristic polynomial (upon substitution $a_s(t)=\xi\exp(-\mathrm{i}\lambda t)$)

$$\lambda^3 + 2\Delta\lambda^2 + (\Delta^2 - \kappa^2 + \Gamma^2)\lambda + \Gamma^2\Delta, \quad \kappa \neq 0, \tag{7.48}$$

is a cubic polynomial in λ with real coefficients. An oscillatory behavior of the signal mode occurs only provided the polynomial (7.48) has three real roots (*casus irreducibilis*), i.e., if its determinant D obeys the condition $D < 0$. Expanding the determinant in the small nonlinear coupling parameter Γ and keeping terms up to the second order in Γ we obtain

$$D \sim -\frac{\kappa^2}{27}\left[(\kappa^2 - \Delta^2)^2 - (5\Delta^2 + 3\kappa^2)\Gamma^2\right], \quad \Gamma \ll \Delta, \kappa. \tag{7.49}$$

It is seen that a mismatched down-conversion behaves in either an oscillatory or a hyperbolic way, depending on the strength of the coupling with the auxiliary mode. The values of κ lying at the boundary between these two types of dynamics are determined by solving the equation $D = 0$. The only two nontrivial solutions are

$$\kappa_{1,2} = \sqrt{\Delta^2 + \frac{3}{2}\Gamma^2 \pm \sqrt{8}\Delta\Gamma}. \tag{7.50}$$

The case $\Delta \gg \Gamma$ is of main interest here. Hence we can, eventually, drop Γ^2 in eq. (7.50). The resulting intervals are

$$\begin{aligned} &\text{hyperbolic behavior:} && \kappa \in \langle \Delta - \sqrt{2}\Gamma, \Delta + \sqrt{2}\Gamma\rangle, \\ &\text{oscillatory behavior:} && \kappa \in \langle 0, \Delta - \sqrt{2}\Gamma\rangle \cup (\Delta + \sqrt{2}\Gamma, \infty). \end{aligned} \tag{7.51}$$

The behavior of the mismatched down-conversion process is shown in fig. 14a for a particular choice of Δ. In absence of linear coupling the down-converted light shows oscillations and the overall effectiveness of the nonlinear process is small due to the presence of phase mismatch Δ. However, as we switch on the coupling between the idler and auxiliary mode, the situation changes. By increasing the strength κ of the coupling the period of the oscillations gets longer and their amplitude larger. When κ becomes larger than $\Delta - \sqrt{2}\Gamma$, the oscillations are no longer seen and the intensity of the signal beam starts to grow monotonously. We can say that in this regime the initial nonlinear mismatch has been compensated by the coupling.

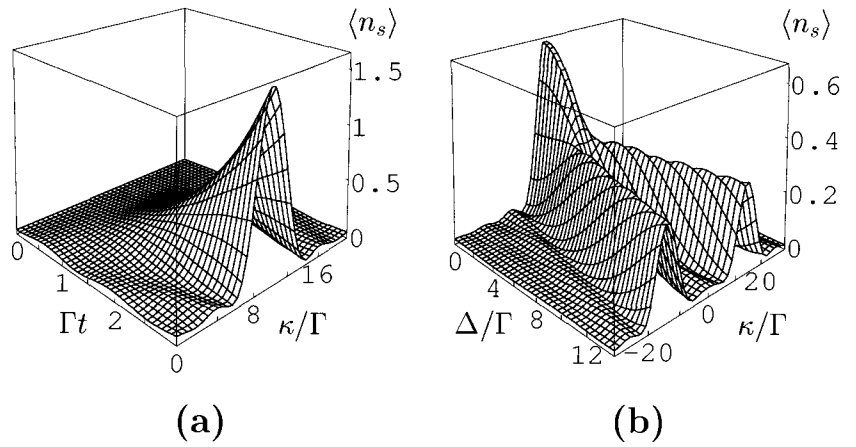

Fig. 14. (a) Mean number of signal photons $\langle n_s \rangle$ behind the nonlinear medium as a function of interaction length t and strength κ of the linear coupling. The nonlinear mismatch is Δ=10Γ. (b) Interplay between linear coupling and phase mismatch. The mean number of signal photons $\langle n_s \rangle$ behind the nonlinear medium of length Γt = 1.5 is shown versus the strength κ of the linear coupling and the nonlinear mismatch Δ. A significant production of signal photons, viewed as a "decay" of the initial state (vacuum), is a clear manifestation of an inverse Zeno effect.

The interplay between nonlinear mismatch and linear coupling is illustrated in fig. 14b. A significant production of signal photons is a clear manifestation of IZE. In accord with the observations of Luis and Sánchez-Soto [1998] and Thun and Peřina [1998], such an IZE occurs only if a substantial phase mismatch is introduced in the process of down-conversion. This is the condition (7.32) for having $\mathcal{Z} < 1$ in the decay of the vacuum state. It is worth comparing the interesting behavior seen in fig. 14b with the Zeno and inverse Zeno effects in a sliced nonlinear crystal discussed in § 7.3. The coupling parameter κ here plays a role similar to the number of slices N, so that one can state again that $\kappa \sim \sqrt{N}$ in the sense of § 5.

7.5. *Dressed modes*

We now look for the modes dressed by the interaction κ. This will provide an alternative interpretation and a more rigorous explanation of the result obtained above. Let us diagonalize the Hamiltonian (7.39) with respect to the linear coupling. It is easy to see that in terms of the dressed modes

$$c = (a_i + b)/\sqrt{2}, \qquad d = (a_i - b)/\sqrt{2}, \tag{7.52}$$

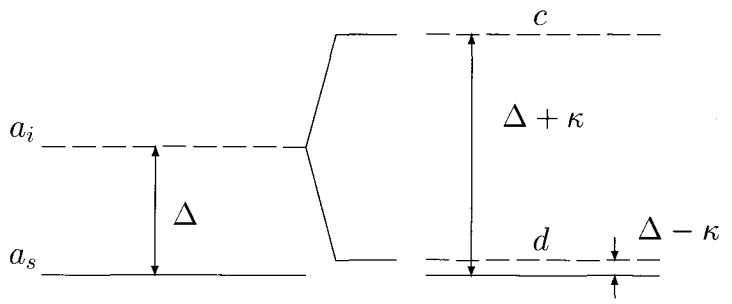

Fig. 15. Energy scheme of a mismatched down-conversion process subject to linear coupling. The bottom solid lines denote a resonant process.

the Hamiltonian (7.39) reads

$$H_\kappa = \omega_c c^\dagger c + \omega_d d^\dagger d + \frac{\Gamma}{\sqrt{2}}(a_s^\dagger c^\dagger + a_s c) + \frac{\Gamma}{\sqrt{2}}(a_s^\dagger d^\dagger + a_s d), \tag{7.53}$$

where the dressed energies are

$$\omega_c = \Delta + \kappa, \qquad \omega_d = \Delta - \kappa. \tag{7.54}$$

The coupling of the idler mode a_i with the auxiliary mode b yields two dressed modes c and d that the pump photon can decay to. They are completely decoupled and due to their energy shift (7.54), exhibit a phase mismatch $\Delta \pm \kappa$. Since the phase mismatch effectively shortens the time during which a fixed-phase relation holds between the interacting beams, the amount of converted energy is smaller than in the ideal case of perfectly phase-matched interaction, $\Delta = 0$. A strong linear coupling then makes the subsequent emissions of converted photons interfere destructively and the nonlinear interaction is frozen. In this respect the disturbances caused by the coupling and by frequently repeated measurements are similar and we can interpret the phenomenon as a QZE. The energy scheme implied by the Hamiltonian (7.53) is shown in fig. 15. Under the influence of the coupling with the auxiliary mode b the mismatched down-conversion splits into two dressed energy–shifted interactions. It is apparent that when $\kappa = \pm\Delta$, one of the two interactions becomes resonant. The other one is "counter-rotating" and acquires a phase mismatch 2Δ, yielding oscillations. Also, the amplitude of such oscillations decreases as Δ^{-2} and the mode output becomes negligible compared to the other one. The use of the rotating wave

approximation in eq. (7.53) is fully justified in this case and the system is easily solved. The output signal intensity reads

$$\langle a_s^\dagger(t)a_s(t)\rangle = \sinh^2\left(\frac{\Gamma}{\sqrt{2}}t\right) \quad (\kappa = \pm\Delta,\ \Delta t \gg 1) \tag{7.55}$$

(compare with eq. 7.7). The linear coupling to an auxiliary mode compensates for the phase mismatch up to a change in the effective nonlinear coupling strength $\Gamma \to \Gamma/\sqrt{2}$.

As a matter of fact, the condition $\kappa = \pm\Delta$ can also be interpreted as a condition for achieving the so-called quasi-phase-matching in the nonlinear process. A quasi-phase-matched regime of generation (Armstrong, Bloembergen, Ducuing and Pershan [1962], Fejer, Magel, Jundt and Byer [1992], Chirkin and Volkov [1998]) is usually forced by creating an artificial lattice inside a nonlinear medium, e.g., by periodic modulation of the nonlinear coupling coefficient. A periodic change of sign of Γ (rectangular modulation) yields the effective coupling strength $\Gamma \to 2\Gamma/\pi$, where, as before, Γ is the coupling strength of the phase-matched interaction. Thus the continuous "observation" of the idler mode even gives a slightly better enhancement of the decay rate than the most common quasi-phase-matching technique.

To summarize, the statement "the down-conversion process is mismatched" means that the nonlinear process is out of resonance in the sense that the momentum of the decay products (signal and idler photons) differs from the momentum carried by the pump photon before the decay took place. When the linear interaction is switched on, the system gets dressed and the energy spectrum changes. A careful adjustment of the coupling strength κ makes it possible to tune the nonlinear interaction back to resonance. In this way the probability of pump photon decay can be greatly enhanced. This occurs when $\kappa \simeq \pm\Delta$ and explains why the inverse Zeno effect takes place along the lines $\kappa = \pm\Delta$ in fig. 14b.

In some sense, on very general grounds, the Zeno effect is a consequence of the new dynamical features introduced by the coupling with an external agent that (through its interaction) "looks closely" at the system. When this interaction can be effectively described as a projection operator à la von Neumann, we obtain the usual formulation of the quantum Zeno effect in the limit of very frequent measurements. In general, the description in terms of projection operators may not apply, but the dynamics can be modified in such a way that an interpretation in terms of Zeno or inverse Zeno effect is appealing and intuitive. This is the main reason why we think that examples of the type analyzed in this chapter call for a broader definition of Zeno effects.

§ 8. Genuine unstable systems and Zeno effects

We will now study the Zeno–inverse Zeno transition in greater detail, by making use of a quantum field theoretical framework, and discuss the primary role played by the form factors of the interaction. As usual, rather than analyzing the general case, we shall focus on simple examples.

We generalize the two-level Hamiltonian (2.1) to N states $|j\rangle$ $(j = 1,\dots,N)$

$$H_{\rm I} = \sum_{j=1}^{N} \Omega_j(|+\rangle\langle j| + |j\rangle\langle +|) = \begin{pmatrix} 0 & \Omega_1 & \dots & \Omega_N \\ \Omega_1 & 0 & \dots & 0 \\ \vdots & \vdots & \vdots & \vdots \\ \Omega_N & 0 & \dots & 0 \end{pmatrix} \tag{8.1}$$

and introduce different energies

$$H_0 = \omega_0|+\rangle\langle +| + \sum_{j=1}^{N} \omega_j|j\rangle\langle j| = \begin{pmatrix} \omega_0 & 0 & \dots & 0 \\ 0 & \omega_1 & \dots & 0 \\ \vdots & \vdots & \vdots & \vdots \\ 0 & 0 & \dots & \omega_N \end{pmatrix}. \tag{8.2}$$

In order to obtain a truly unstable system we need a continuous spectrum, so we will consider the continuum limit of these Hamiltonians

$$H = H_0 + H_{\rm I} = \omega_0|+\rangle\langle +| + \int \mathrm{d}\omega\ \omega|\omega\rangle\langle\omega| + \int \mathrm{d}\omega\ g(\omega)(|+\rangle\langle\omega| + |\omega\rangle\langle +|). \tag{8.3}$$

The transition to a quantum field theoretical framework is an important component of our analysis, as we shall see. As before, we take as the initial state $|\psi_0\rangle = |+\rangle$. The interaction of this normalizable state with the continuum of states $|\omega\rangle$ is responsible for its decay and depends on the *form factor* $g(\omega)$. We reobtain the physics of two-level systems in the limit $g^2(\omega) = \Omega^2\delta(\omega)$.

The Fourier–Laplace transform of the survival amplitude for this model can be given a convenient analytic expression. Notice that the transform of the survival amplitude is the expectation value of the resolvent

$$\mathcal{A}(E) = \int_0^\infty \mathrm{d}t\ \mathrm{e}^{\mathrm{i}Et}\mathcal{A}(t) = \langle +| \int_0^\infty \mathrm{d}t\ \mathrm{e}^{\mathrm{i}Et}\mathrm{e}^{-\mathrm{i}Ht}|+\rangle = \langle +|\frac{\mathrm{i}}{E-H}|+\rangle, \tag{8.4}$$

and is defined for $\mathrm{Im}\,E > 0$. By using twice the operator identity

$$\frac{1}{E-H} = \frac{1}{E-H_0} + \frac{1}{E-H_0}H_{\rm I}\frac{1}{E-H} \tag{8.5}$$

one obtains

$$\mathcal{A}(E) = \langle +| \left[\frac{\mathrm{i}}{E-H_0} + \frac{1}{E-H_0} H_\mathrm{I} \frac{\mathrm{i}}{E-H_0} + \frac{1}{E-H_0} H_\mathrm{I} \frac{1}{E-H_0} H_\mathrm{I} \frac{\mathrm{i}}{E-H} \right] |+\rangle$$
$$= \frac{\mathrm{i}}{E-\omega_0} + \frac{1}{E-\omega_0} \int \mathrm{d}\omega \, \frac{|\langle +|H_\mathrm{I}|\omega\rangle|^2}{E-\omega} \, \mathcal{A}(E). \tag{8.6}$$

In the above derivation we used the fact that H_I is completely off-diagonal in the eigenbasis of H_0, $\{|+\rangle, |\omega\rangle\}$, which is a resolution of the identity

$$|+\rangle\langle +| + \int \mathrm{d}\omega \, |\omega\rangle\langle\omega| = 1. \tag{8.7}$$

The algebraic equation (8.6) can be solved and gives

$$\mathcal{A}(E) = \frac{\mathrm{i}}{E - \omega_0 - \Sigma(E)}, \tag{8.8}$$

where the self-energy function $\Sigma(E)$ is related to the form factor $g(\omega)$ by a simple integration

$$\Sigma(E) = \int \mathrm{d}\omega \, \frac{|\langle +|H_\mathrm{I}|\omega\rangle|^2}{E-\omega} = \int \mathrm{d}\omega \, \frac{g^2(\omega)}{E-\omega}. \tag{8.9}$$

By inverting eq. (8.4) we finally get

$$\mathcal{A}(t) = \int_\mathrm{B} \frac{\mathrm{d}E}{2\pi} \, \mathrm{e}^{-\mathrm{i}Et} \mathcal{A}(E) = \frac{\mathrm{i}}{2\pi} \int_\mathrm{B} \mathrm{d}E \, \frac{\mathrm{e}^{-\mathrm{i}Et}}{E - \omega_0 - \Sigma(E)}, \tag{8.10}$$

the Bromwich path B being a horizontal line $\mathrm{Im}\, E$ = constant > 0 in the half plane of convergence of the Fourier-Laplace transform (upper-half plane).

We consider now a particular case. Let the form factor be Lorentzian

$$g(\omega) = \frac{\Omega}{\sqrt{\pi}} \sqrt{\frac{\Lambda}{\omega^2 + \Lambda^2}}. \tag{8.11}$$

This describes, for instance, an atom-field coupling in a cavity with high finesse mirrors (Lang, Scully and Lamb [1973], Ley and Loudon [1987], Gea-Banacloche, Lu, Pedrotti, Prasad, Scully and Wodkiewicz [1990]). (Notice that

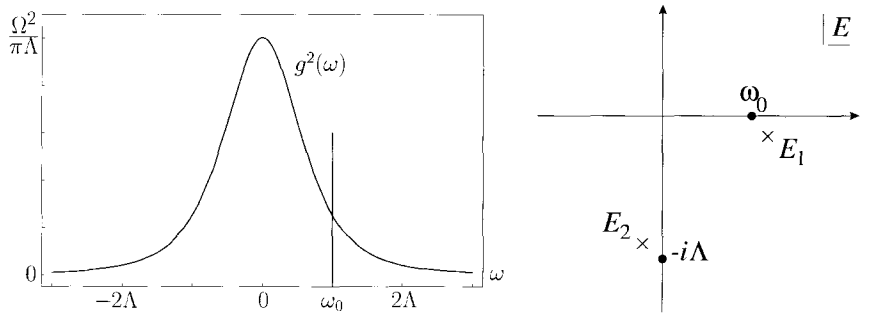

Fig. 16. (a) Form factor $g^2(\omega)$ and position of the initial state energy ω_0. (b) Poles of the propagator in the complex E-plane.

the Hamiltonian in this case is not lower bounded and we expect no deviations from exponential behavior at very large times.) In this case one easily obtains

$$\Sigma(E) = \frac{\Omega^2}{E + \mathrm{i}\Lambda}, \tag{8.12}$$

whence the propagator

$$\mathcal{A}(E) = \frac{\mathrm{i}(E + \mathrm{i}\Lambda)}{(E-\omega_0)(E+\mathrm{i}\Lambda) - \Omega^2}, \tag{8.13}$$

has two poles in the lower-half energy plane (see fig. 16). Their values are

$$E_1 = \omega_0 + \Delta - \mathrm{i}\frac{\gamma}{2}, \quad E_2 = -\Delta - \mathrm{i}\left(\Lambda - \frac{\gamma}{2}\right), \tag{8.14}$$

where

$$\begin{cases} \Delta = -\frac{\omega_0}{2} + \frac{\omega_0}{2} \sqrt{\frac{\sqrt{\varsigma^4 + 4\omega_0^2\Lambda^2} + \varsigma^2}{2\omega_0^2}}, \\ \gamma = \Lambda - \sqrt{\frac{\sqrt{\varsigma^4 + 4\omega_0^2\Lambda^2} - \varsigma^2}{2}}, \end{cases} \quad \text{with} \quad \varsigma^2 = \omega_0^2 + 4\Omega^2 - \Lambda^2. \tag{8.15}$$

(Notice that ς^2 can be negative.) The survival amplitude reads

$$\mathcal{A}(t) = \frac{E_1 + \mathrm{i}\Lambda}{E_1 - E_2} \mathrm{e}^{-\mathrm{i}E_1 t} - \frac{E_2 + \mathrm{i}\Lambda}{E_1 - E_2} \mathrm{e}^{-\mathrm{i}E_2 t}$$
$$= \frac{\omega_0 + \Delta + \mathrm{i}(\Lambda - \gamma/2)}{\omega_0 + 2\Delta + \mathrm{i}(\Lambda - \gamma)} \mathrm{e}^{-\mathrm{i}(\omega_0 + \Delta)t} \mathrm{e}^{-\gamma t/2}$$
$$+ \frac{\Delta - \mathrm{i}\gamma/2}{\omega_0 + 2\Delta + \mathrm{i}(\Lambda - \gamma)} \mathrm{e}^{\mathrm{i}\Delta t} \mathrm{e}^{-(\Lambda - \gamma/2)t}$$
$$= (1 - \mathcal{R}) \mathrm{e}^{-\mathrm{i}(\omega_0 + \Delta)t} \mathrm{e}^{-\gamma t/2} + \mathcal{R} \mathrm{e}^{\mathrm{i}\Delta t} \mathrm{e}^{-(\Lambda - \gamma/2)t}, \tag{8.16}$$

where

$$1-\mathcal{R} = -\mathrm{i}\mathrm{Res}[\mathcal{A}(E_1)] = \frac{1}{1-\Sigma'(E_1)} = \frac{\omega_0+\Delta+\mathrm{i}(\Lambda-\gamma/2)}{\omega_0+2\Delta+\mathrm{i}(\Lambda-\gamma)} \tag{8.17}$$

is the residue of the pole $E_1 = \omega_0 + \Delta - \mathrm{i}\gamma/2$ of the propagator. The survival probability reads

$$P(t) = |\mathcal{A}(t)|^2 = \mathcal{Z}\exp(-\gamma t) + 2\,\mathrm{Re}[\mathcal{R}^*(1-\mathcal{R})\,\mathrm{e}^{-\mathrm{i}(\omega_0+2\Delta)t}]\exp(-\Lambda t) + |\mathcal{R}|^2\exp[-(2\Lambda-\gamma)t], \tag{8.18}$$

where $\mathcal{Z} = |1-\mathcal{R}|^2$ is the wave function renormalization. We now focus on the Zeno–inverse Zeno transition and the conditions for it to take place. The reader should refer to the discussion of § 3.2. For the sake of simplicity, we consider the weak coupling limit $\Omega \ll \omega_0, \Lambda$, where one obtains

$$\Delta = \mathrm{P}\int \mathrm{d}\omega \frac{g^2(\omega)}{\omega_0-\omega} + \mathrm{O}(\Omega^4) = \frac{\Omega^2}{\omega_0^2+\Lambda^2}\omega_0 + \mathrm{O}(\Omega^4),$$
$$\gamma = 2\pi g^2(\omega_0) + \mathrm{O}(\Omega^4) = 2\Lambda\frac{\Omega^2}{\omega_0^2+\Lambda^2} + \mathrm{O}(\Omega^4). \tag{8.19}$$

Notice that the latter formula is the Fermi "golden" rule. The second exponential in eq. (8.16) is damped very quickly, on a time scale Λ^{-1} much faster than γ^{-1}, whence, after a short initial quadratic (Zeno) region of duration Λ^{-1}, the decay becomes purely exponential with decay rate γ. Notice that the corrections are of order Ω^2

$$\mathcal{R} = \frac{\Omega^2}{\omega_0^2+\Lambda^2}\frac{\omega_0-\mathrm{i}\Lambda}{\omega_0+\mathrm{i}\Lambda} + \mathrm{O}(\Omega^4) \tag{8.20}$$

and the Zeno time is $\tau_Z = \Omega^{-1} \gg \Lambda^{-1}$, i.e., the initial quadratic (Zeno) region is much shorter than the Zeno time. In general, the Zeno time does *not* yield a correct estimate of the duration of the Zeno region. The approximation $P(t) \simeq 1 - t^2/\tau_Z^2$ (see eq. 3.3) holds for times $t < \Lambda^{-1} \ll \tau_Z$. According to § 3.2, a sufficient condition for the system to exhibit a Zeno–inverse Zeno transition is $\mathcal{Z} < 1$, which in our case reads

$$\mathcal{Z} = 1 - 2\frac{\Omega^2}{\omega_0^2+\Lambda^2}\,\mathrm{Re}\left[\frac{\omega_0-\mathrm{i}\Lambda}{\omega_0+\mathrm{i}\Lambda}\right] + \mathrm{O}(\Omega^4) = 1 - 2\frac{\Omega^2}{\omega_0^2+\Lambda^2}\frac{\omega_0^2-\Lambda^2}{\omega_0^2+\Lambda^2} + \mathrm{O}(\Omega^4) < 1, \tag{8.21}$$

namely

$$\omega_0^2 > \Lambda^2 + \mathrm{O}(\Omega^2). \tag{8.22}$$

This is a condition of asymmetry of the initial energy ω_0 with respect to the form factor (see fig. 16). Notice that in atomic or molecular systems coupled to the free space photon vacuum this condition is always extremely well satisfied (Facchi and Pascazio [1998]). In such a case, namely, if $\omega_0^2 \gg \Lambda^2$, the transition time is well approximated by eq. (3.13), which yields (remember eq. 3.15)

$$\tau^* \simeq \gamma\tau_Z^2 = \frac{2\Lambda}{\omega_0^2+\Lambda^2} + \mathrm{O}(\Omega^2). \tag{8.23}$$

When ω_0 gets closer to the peak of the form factor, the effective decay rates $\gamma_{\mathrm{eff}}(\tau)$ in eq. (3.12) are not linear in τ anymore and the solution τ^* of the equation $\gamma_{\mathrm{eff}}(\tau^*) = \gamma$ becomes larger than the approximation (8.23), eventually going to infinity when the condition (8.22) is no longer valid. In such a case, only a QZE is possible. This situation is outlined in fig. 17, where the effective decay rate $\gamma_{\mathrm{eff}}(\tau)$ is displayed for different values of the ratio ω_0/Λ. The conclusions drawn for the Lorentzian model (8.11) are of general validity (Facchi, Nakazato and Pascazio [2001]). The occurrence of a Zeno–inverse Zeno transition depends on the form factor of the coupling and on the ratio $(\omega_0 - \omega_g)/\Lambda$, where ω_g is the energy of the ground state. We will not go into additional details here.

It is interesting to consider some limits of the model investigated. In the limit

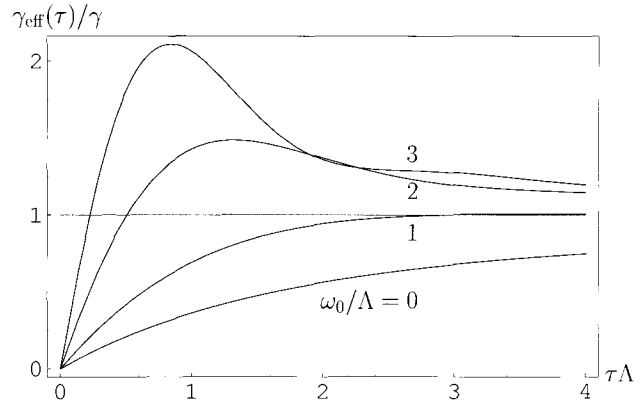

Fig. 17. Effective decay rate $\gamma_{\mathrm{eff}}(\tau)$ for the model (8.11), for $\lambda = 0.1$ and different values of the ratio ω_0/Λ (indicated). The horizontal line shows the "natural" decay rate γ: its intersection with $\gamma_{\mathrm{eff}}(\tau)$ yields the solution τ^* of eq. (3.15). The asymptotic value of all curves is γ, as expected. A Zeno (inverse Zeno) effect is obtained for $\tau < \tau^*$ ($\tau > \tau^*$). Notice the presence of a linear region for small values of τ and observe that τ^* does not belong to such linear region as the ratio ω_0/Λ decreases. Above a certain threshold, given by eq. (8.22) in the weak coupling limit of the model (and in general by the condition $\mathcal{Z} = 1$), eq. (3.15) has no finite solutions: only a Zeno effect is realizable in such a case.

of large bandwidth $\Lambda \gg \omega_0, \Omega$, from eq. (8.15) one gets $\gamma = 2\Omega^2/\Lambda + O(\Lambda^{-2})$ and in order to have a nontrivial result with a finite decay rate, we let

$$\Lambda \to \infty, \quad \Omega \to \infty, \qquad \text{with} \quad \frac{\Omega^2}{\Lambda} = \frac{\gamma}{2} = \text{const.} \tag{8.24}$$

In this limit the continuum has a flat band, $g(\omega) = \sqrt{\gamma/2\pi}$ =const, and we expect to recover the results of § 5.2. Indeed, in this case one gets $\mathcal{R} = 0$ and $\Delta = 0$, whence

$$\mathcal{A}(E) = \frac{\mathrm{i}}{E - \omega_0 + \mathrm{i}\gamma/2}, \tag{8.25}$$

so that the survival amplitude and probability read

$$\mathcal{A}(t) = \exp\left(-\mathrm{i}\omega_0 t - \frac{\gamma}{2}t\right) \quad \text{and} \quad P(t) = \exp(-\gamma t). \tag{8.26}$$

In this case the propagator (8.25) has only a simple pole and the survival probability (8.26) is purely exponential. Therefore measurements cannot modify the free behavior. Indeed, the conditions for occurrence of a Zeno effect are always ascribable to the presence of an initial non-exponential behavior of the survival probability, which is caused by a propagator exhibiting a richer structure than a simple pole in the complex energy plane.

In the limit of narrow bandwidth $\Lambda \ll \omega_0, \Omega$, the form factor becomes

$$g^2(\omega) = \Omega^2 \delta(\omega) \tag{8.27}$$

and the continuum is "concentrated" in $\omega = 0$. Therefore the continuum behaves as a second discrete level and one obtains Rabi oscillations. In fact one gets

$$\gamma = 0, \quad \Delta = -\frac{\omega_0}{2} + \Omega_1, \quad \mathcal{R} = \tfrac{1}{2}\left(1 - \frac{\omega_0}{2\Omega_1}\right), \tag{8.28}$$

where

$$\Omega_1 = \sqrt{\Omega^2 + \frac{\omega_0^2}{4}} \tag{8.29}$$

is the usual Rabi frequency of a two-level system with energy difference ω_0 and coupling Ω. By (8.28) the survival amplitude and probability read

$$\begin{aligned} \mathcal{A}(t) &= \tfrac{1}{2}\left(1 + \frac{\omega_0}{2\Omega_1}\right) \mathrm{e}^{-\mathrm{i}(\omega_0 + \Omega_1)t} + \tfrac{1}{2}\left(1 - \frac{\omega_0}{2\Omega_1}\right) \mathrm{e}^{-\mathrm{i}(\omega_0 - \Omega_1)t}, \\ P(t) &= 1 - \frac{\Omega^2}{\Omega_1^2} \sin^2\left(\frac{\Omega_1 t}{2}\right). \end{aligned} \tag{8.30}$$

In this case, if $\omega_0 = 0$ (initial state energy at the center of the form factor), the survival probability (8.30) oscillates between 1 and 0 and only a QZE is possible. On the other hand, if $\omega_0 \neq 0$ (initial state energy strongly asymmetric with respect to the form factor of "width" $\Lambda = 0$) the initial state never decays completely. By measuring the system, the survival probability will vanish exponentially, independently of the strength of observation, whence only an IZE is possible. This is what we found for a down-conversion process with a sufficiently large phase mismatch at the end of § 7.2.

Incidentally, notice that the Zeno time is still $\tau_Z = \Omega^{-1}$ and now yields a good estimate of the duration of the Zeno region. This is, so to say, a "coincidence" due to the oscillatory features of the system.

Another interesting case is that of strong coupling, $\Omega \simeq \Lambda$. Roughly speaking, it yields the situation outlined in fig. 6b. This is a typical case in which the strong coupling provokes violent oscillations before the system reaches the asymptotic regime. In the limit $\Omega \gg \Lambda, \omega_0$, we get

$$\Delta = \Omega - \frac{\omega_0}{2} + O(\Omega^{-1}), \quad \gamma = -\mathrm{i}\frac{\Lambda}{2} + O(\Omega^{-1}), \quad \mathcal{R} = \frac{1}{2} - \frac{\omega_0 + \mathrm{i}\Lambda}{4\Omega} + O(\Omega^{-3}), \tag{8.31}$$

whence the survival amplitude reads

$$\mathcal{A}(t) \simeq \exp\left(-\mathrm{i}\frac{\omega_0}{2}t - \frac{\Lambda}{2}t\right)\left[\left(\frac{1}{2} + \frac{\omega_0 + \mathrm{i}\Lambda}{4\Omega}\right)\mathrm{e}^{-\mathrm{i}\Omega t} + \left(\frac{1}{2} - \frac{\omega_0 + \mathrm{i}\Lambda}{4\Omega}\right)\mathrm{e}^{\mathrm{i}\Omega t}\right], \tag{8.32}$$

which yields fast oscillations of frequency Ω damped at a rate $\Lambda \ll \Omega$.

Finally, let us comment on the issue of continuous measurement. This is accomplished, for instance, by adding to (8.3) the following Hamiltonian:

$$H_{\text{meas}}(\Gamma) = \sqrt{\frac{\Gamma}{2\pi}} \int \mathrm{d}\omega\, \mathrm{d}\omega'\, (|\omega\rangle\langle\omega, \omega'| + |\omega, \omega'\rangle\langle\omega|) + \int \mathrm{d}\omega'\, |\omega'\rangle\langle\omega'|. \tag{8.33}$$

As soon as a photon is emitted, it is coupled to another boson of frequency ω' (notice that the coupling has no form factor). By following a reasoning identical to that of § 5.2, one can show that the dynamics of the Hamiltonian (8.3)–(8.33), in the relevant subspace, is generated by

$$H = \omega_0 |+\rangle\langle+| + \int \mathrm{d}\omega\, (\omega - \mathrm{i}\Gamma/2)|\omega\rangle\langle\omega| + \int \mathrm{d}\omega\, g(\omega)(|+\rangle\langle\omega| + |\omega\rangle\langle+|), \tag{8.34}$$

and an effective continuous observation on the system is obtained by increasing Γ. Indeed it is easy to see that the only effect due to Γ in eq. (8.34) is the substitution of $\Sigma(E)$ with $\Sigma(E + \mathrm{i}\Gamma/2)$ in eq. (8.8), namely,

$$\mathcal{A}(E) = \frac{\mathrm{i}}{E - \omega_0 - \Sigma(E + \mathrm{i}\Gamma/2)}. \tag{8.35}$$

For large values of Γ, i.e., for very quick response of the "apparatus", the self-energy function (8.9) has the asymptotic behavior

$$\Sigma\left(E+\mathrm{i}\frac{\Gamma}{2}\right) \sim -\mathrm{i}\frac{2}{\Gamma}\int \mathrm{d}\omega\, g^2(\omega) = -\mathrm{i}\frac{2}{\Gamma\tau_Z^2}, \quad \text{for} \quad \Gamma \to \infty, \tag{8.36}$$

where the definition of $g(\omega)$ was used,

$$\int \mathrm{d}\omega\, g^2(\omega) = \int \mathrm{d}\omega\, |\langle +|H_I|\omega\rangle|^2 = \langle +|H_I^2|+\rangle = \frac{1}{\tau_Z^2}. \tag{8.37}$$

[Notice that $\Gamma \to \infty$ in (8.36) means $\Gamma \gg \Lambda$, the frequency cutoff of the form factor.] In this case the propagator (8.35) reads

$$\mathcal{A}(E) \sim \frac{\mathrm{i}}{E-\omega_0+\mathrm{i}\gamma_{\mathrm{eff}}(\Gamma)/2}, \quad \text{for} \quad \Gamma \to \infty, \tag{8.38}$$

and the survival probability decays with the effective exponential rate (valid for $\Gamma \gg \Lambda$)

$$\gamma_{\mathrm{eff}}(\Gamma) = \frac{4}{\tau_Z^2\Gamma}. \tag{8.39}$$

The effective rate (8.39) is the same result (5.12) we found for the particular model considered in § 5.2. We see that it is a general result. The equivalence (5.13) is therefore of general validity. Additionally, we have here a scale for the validity of the linear approximation for γ_{eff}. The linear term in the asymptotic expansion (8.36) approximates well the self-energy function only for values of Γ that are larger than the bandwidth Λ. For smaller values of Γ one has to take into account the nonlinearities arising from the successive terms in the expansion.

Note that the flat-band case (8.25), yielding a purely exponential decay, is also unaffected by the continuous measurement. Indeed in that case $\Sigma(E) = -\mathrm{i}\gamma/2$ is a constant independent of E, whence $\Sigma(E + i\Gamma/2) = \Sigma(E)$ is independent of Γ. The same thing happens if one considers the Weisskopf–Wigner approximation. In this case one neglects the whole structure of the propagator in the complex energy plane and retains only the dominant pole near the real axis. This yields, as we have seen, a self-energy function which does not depend on energy and a purely exponential decay (without any deviations), that cannot be modified by any observations.

Notice that the very existence of a QZE is related to the existence of an initial quadratic behavior of the survival probability, i.e., to a finite value of τ_Z.

As eq. (8.37) shows, this is related to the convergence of the integral of the form factor. In general, in a quantum field theoretical framework, the Zeno time τ_Z (the inverse of the second moment of the Hamiltonian) cannot be defined, because it vanishes for pointlike particles. It becomes necessary to introduce form factors and cutoffs and use more sophisticated techniques. These problems will not be discussed here. See Bernardini, Maiani and Testa [1993], Facchi and Pascazio [1998], Joichi, Matsumoto and Yoshimura [1998], Maiani and Testa [1998], Alvarez-Estrada and Sánchez-Gómez [1999].

§ 9. Three-level system in a laser field

We shall now investigate a realistic situation in which a continuous observation performed by a laser field leads to an inverse Zeno effect, in a way very similar to that outlined in § 5. We shall look at the temporal behavior of a three-level system (such as an atom or a molecule), where level $|1\rangle$ is the ground state and levels $|2\rangle$, $|3\rangle$ are two excited states. (See fig. 18.) The system is initially prepared in level $|2\rangle$ and if it follows its natural evolution, it will decay to level $|1\rangle$. The decay will be (approximately) exponential and characterized by a certain lifetime, that can be calculated from the Fermi golden rule. But if one shines an intense laser field on the system, tuned at the transition frequency 3-1, the evolution can be different. This problem was investigated by Mihokova, Pascazio and Schulman [1997], who found that the lifetime of the initial state depends on the intensity of the laser field. We shall see that for physically sensible values of the intensity of the laser, the decay is *enhanced*. This can be viewed as an inverse quantum Zeno effect (Facchi and Pascazio [2000], Pascazio and Facchi [1999]). An important role will be played by the form factor of the interaction Hamiltonian.

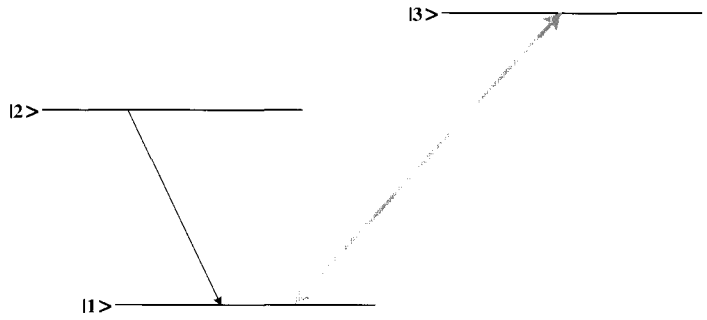

Fig. 18. Level configuration.

9.1. *The system*

We consider the Hamiltonian ($\hbar = c = 1$)

$$\begin{aligned} H &= H_0 + H_{\text{int}} \\ &= \omega_0 |2\rangle\langle 2| + \Omega_0 |3\rangle\langle 3| + \sum_{\boldsymbol{k},\lambda} \omega_k a^\dagger_{\boldsymbol{k}\lambda} a_{\boldsymbol{k}\lambda} + \sum_{\boldsymbol{k},\lambda} \left(\phi_{\boldsymbol{k}\lambda} a^\dagger_{\boldsymbol{k}\lambda} |1\rangle\langle 2| + \phi^*_{\boldsymbol{k}\lambda} a_{\boldsymbol{k}\lambda} |2\rangle\langle 1| \right) \\ &\quad + \sum_{\boldsymbol{k},\lambda} \left(\Phi_{\boldsymbol{k}\lambda} a^\dagger_{\boldsymbol{k}\lambda} |1\rangle\langle 3| + \Phi^*_{\boldsymbol{k}\lambda} a_{\boldsymbol{k}\lambda} |3\rangle\langle 1| \right), \end{aligned} \tag{9.1}$$

where the first two terms are the free Hamiltonian of the 3-level atom (whose states $|i\rangle$ ($i = 1, 2, 3$) have energies $E_1 = 0$, $\omega_0 = E_2 - E_1 > 0$, $\Omega_0 = E_3 - E_1 > 0$), the third term is the free Hamiltonian of the EM field and the last two terms describe the $1 \leftrightarrow 2$ and $1 \leftrightarrow 3$ transitions in the rotating wave approximation, respectively. (See fig. 18.) States $|2\rangle$ and $|3\rangle$ are chosen so that no transition between them is possible (e.g., because of selection rules). The matrix elements of the interaction Hamiltonian read

$$\begin{aligned} \phi_{\boldsymbol{k}\lambda} &= \frac{e}{\sqrt{2\epsilon_0 V \omega}} \int \mathrm{d}^3x \, \mathrm{e}^{-\mathrm{i}\boldsymbol{k}\cdot\boldsymbol{x}} \boldsymbol{\epsilon}^*_{\boldsymbol{k}\lambda} \cdot \boldsymbol{j}_{12}(\boldsymbol{x}) \\ \Phi_{\boldsymbol{k}\lambda} &= \frac{e}{\sqrt{2\epsilon_0 V \omega}} \int \mathrm{d}^3x \, \mathrm{e}^{-\mathrm{i}\boldsymbol{k}\cdot\boldsymbol{x}} \boldsymbol{\epsilon}^*_{\boldsymbol{k}\lambda} \cdot \boldsymbol{j}_{13}(\boldsymbol{x}), \end{aligned} \tag{9.2}$$

where $-e$ is the electron charge, ϵ_0 the vacuum permittivity, V the volume of the box, $\omega = |\boldsymbol{k}|$, $\boldsymbol{\epsilon}_{\boldsymbol{k}\lambda}$ the photon polarization and $\boldsymbol{j}_{\text{fi}}$ the transition current of the radiating system. For example, in the case of an electron in an external field, we have $\boldsymbol{j}_{\text{fi}} = \psi^\dagger_{\text{f}} \boldsymbol{\alpha} \psi_{\text{i}}$ where ψ_{i} and ψ_{f} are the wavefunctions of the initial and final state, respectively, and $\boldsymbol{\alpha}$ is the vector of Dirac matrices. For the sake of generality we are using relativistic matrix elements, but our analysis can also be performed with nonrelativistic ones $\boldsymbol{j}_{\text{fi}} = \psi^*_{\text{f}} \boldsymbol{p} \psi_{\text{i}} / m_e$, where $\boldsymbol{p}/m_e$ is the electron velocity.

We shall concentrate on a 3-level system bathed in a continuous laser beam, whose photons have momentum $\boldsymbol{k}_0$ ($|\boldsymbol{k}_0| = \Omega_0$) and polarization λ_0, and assume, throughout this chapter, that

$$\phi_{\boldsymbol{k}_0\lambda_0} = 0, \tag{9.3}$$

i.e., the laser does not interact with state $|2\rangle$. The laser is in a coherent state $|\alpha_0\rangle$ with a very large average number $\bar{N}_0 = |\alpha_0|^2$ of $\boldsymbol{k}_0$-photons in volume V

[we will eventually consider the thermodynamical limit; see eq. (9.21)]. In the picture defined by the unitary operator

$$T(t) = \exp\left(\alpha^*_0 \mathrm{e}^{\mathrm{i}\Omega_0 t} a_{\boldsymbol{k}_0\lambda_0} - \alpha_0 \mathrm{e}^{-\mathrm{i}\Omega_0 t} a^\dagger_{\boldsymbol{k}_0\lambda_0} \right), \tag{9.4}$$

the $\boldsymbol{k}_0$ mode is initially in the vacuum state (Mollow [1975], Cohen-Tannoudji, Dupont-Roc and Grynberg [1998]) and the Hamiltonian becomes ($\bar{N}_0 \gg 1$)

$$\begin{aligned} H \simeq\ & \omega_0 |2\rangle\langle 2| + \Omega_0 |3\rangle\langle 3| + \sum_{\boldsymbol{k},\lambda} \omega_k a^\dagger_{\boldsymbol{k}\lambda} a_{\boldsymbol{k}\lambda} + {\sum_{\boldsymbol{k},\lambda}}' \left(\phi_{\boldsymbol{k}\lambda} a^\dagger_{\boldsymbol{k}\lambda} |1\rangle\langle 2| + \phi^*_{\boldsymbol{k}\lambda} a_{\boldsymbol{k}\lambda} |2\rangle\langle 1| \right) \\ &+ \left(\Phi_{\boldsymbol{k}_0\lambda_0} \alpha^*_0 \mathrm{e}^{\mathrm{i}\Omega_0 t} |1\rangle\langle 3| + \Phi^*_{\boldsymbol{k}_0\lambda_0} \alpha_0 \mathrm{e}^{-\mathrm{i}\Omega_0 t} |3\rangle\langle 1| \right), \end{aligned} \tag{9.5}$$

where a prime means that the summation does not include $(\boldsymbol{k}_0, \lambda_0)$ (due to hypothesis (9.3). In the above equations and henceforth, the vector $|i; n_{\boldsymbol{k}\lambda}\rangle$ represents a state in which the atom is in state $|i\rangle$ and the electromagnetic field in a state with $n_{\boldsymbol{k}\lambda}$ $(\boldsymbol{k}, \lambda)$-photons. We shall analyze the behavior of the system under the action of a continuous laser beam of high intensity. Under these conditions, level configurations similar to that of fig. 18 give rise to the phenomenon of induced transparency (Tewari and Agarwal [1986], Harris, Field and Imamoglu [1990], Boller, Imamoglu and Harris [1991], Field, Hahn and Harris [1991], Zhu, Narducci and Scully [1995], Zhu and Scully [1996], Huang, Zhu, Zubairy and Scully [1996]), for laser beams of sufficiently high intensities. Our interest, however, will be focused on *unstable* initial states. We shall study the temporal behavior of level $|2\rangle$ when the system is shined by a continuous laser of intensity comparable to those used to obtain induced transparency.

The operator

$$\mathcal{N} = |2\rangle\langle 2| + {\sum_{\boldsymbol{k},\lambda}}' a^\dagger_{\boldsymbol{k}\lambda} a_{\boldsymbol{k}\lambda}, \tag{9.6}$$

satisfies

$$[H, \mathcal{N}] = 0, \tag{9.7}$$

which implies the conservation of the total number of photons plus the atomic excitation [Tamm–Dancoff approximation (Tamm [1945], Dancoff [1950])]. The Hilbert space splits therefore into sectors that are invariant under the action of the Hamiltonian. In our case, the system evolves in the subspace labeled by the eigenvalue $\mathcal{N} = 1$ and the analysis can be restricted to this sector (Radmore and Knight [1982], Knight and Lauder [1990]).

9.2. *Schrödinger equation and temporal evolution*

We will study the temporal evolution by solving the time-dependent Schrödinger equation

$$\mathrm{i}\frac{\mathrm{d}}{\mathrm{d}t}|\psi(t)\rangle = H(t)|\psi(t)\rangle, \tag{9.8}$$

where the states of the total system in the sector $\mathcal{N} = 1$ read

$$|\psi(t)\rangle = x(t)|2;0\rangle + \sum_{k,\lambda}{}' y_{k\lambda}(t)|1;1_{k\lambda}\rangle + \sum_{k,\lambda}{}' z_{k\lambda}(t)\mathrm{e}^{-\mathrm{i}\Omega_0 t}|3;1_{k\lambda}\rangle \tag{9.9}$$

and are normalized:

$$\langle\psi(t)|\psi(t)\rangle = |x(t)|^2 + \sum_{k,\lambda}{}' |y_{k,\lambda}(t)|^2 + \sum_{k,\lambda}{}' |z_{k,\lambda}(t)|^2 = 1 \quad (\forall t). \tag{9.10}$$

By inserting (9.9) in (9.8) one obtains the equations of motion

$$\begin{aligned}
&\mathrm{i}\dot{x}(t) = \omega_0 x(t) + \sum_{k,\lambda}{}' \phi^*_{k\lambda}\, y_{k\lambda}(t),\\
&\mathrm{i}\dot{y}_{k\lambda}(t) = \phi_{k\lambda}x(t) + \omega_k y_{k\lambda}(t) + \alpha_0^* \Phi_{k_0\lambda_0} z_{k\lambda}(t),\\
&\mathrm{i}\dot{z}_{k\lambda}(t) = \alpha_0 \Phi^*_{k_0\lambda_0} y_{k\lambda}(t) + \omega_k z_{k\lambda}(t),
\end{aligned} \tag{9.11}$$

where a dot denotes time derivative. At time $t = 0$ we prepare our system in the state

$$|\psi(0)\rangle = |2;0\rangle \quad \Leftrightarrow \quad x(0) = 1,\ y_{k\lambda}(0) = 0,\ z_{k\lambda}(0) = 0. \tag{9.12}$$

By Fourier-Laplace transforming the system of differential equations (9.11) and incorporating the initial conditions (9.12) the solution reads

$$\tilde{x}(E) = \frac{\mathrm{i}}{E - \omega_0 - \Sigma(B,E)}, \tag{9.13}$$

$$\tilde{y}_{k\lambda}(E) = \frac{\phi_{k\lambda}(E - \omega_k)}{(E-\omega_k)^2 - B^2}\,\tilde{x}(E), \tag{9.14}$$

$$\tilde{z}_{k\lambda}(E) = \frac{\sqrt{\bar{N}_0}\Phi^*_{k_0\lambda_0}\phi_{k\lambda}}{(E-\omega_k)^2 - B^2}\,\tilde{x}(E), \tag{9.15}$$

with

$$\Sigma(B,E) = \sum_{k,\lambda} |\phi_{k\lambda}|^2 \frac{E-\omega_k}{(E-\omega_k)^2 - B^2} \tag{9.16}$$

and where

$$B^2 = \bar{N}_0\,|\Phi_{k_0\lambda_0}|^2 \tag{9.17}$$

is proportional to the intensity of the laser field and can be viewed as the "strength" of the observation performed by the laser beam on level $|2\rangle$ (in the

sense of § 5). Note that the coupling B is related to the Rabi frequency by the simple relation $B = \Omega_{\mathrm{Rabi}}/2$.

In the continuum limit ($V \to \infty$), the matrix elements scale as follows

$$\lim_{V\to\infty} \frac{V\omega^2}{(2\pi)^3} \sum_\lambda \int \mathrm{d}\Omega\, |\phi_{k\lambda}|^2 \equiv g^2 \omega_0 \chi^2(\omega), \tag{9.18}$$

where Ω is the solid angle. The (dimensionless) function $\chi(\omega)$ and coupling constant g have the following general properties (Facchi and Pascazio [2000])

$$\chi^2(\omega) \propto \begin{cases} \omega^{2j\mp 1} & \text{if } \omega \ll \Lambda, \\ \omega^{-\beta} & \text{if } \omega \gg \Lambda, \end{cases} \tag{9.19}$$

$$g^2 = \alpha(\omega_0/\Lambda)^{2j+1\mp 1}, \tag{9.20}$$

where j is the total angular momentum of the photon emitted in the $2 \to 1$ transition, $\mp$ represent electric and magnetic transitions, respectively, $\beta(>1)$ is a constant, α the fine structure constant and Λ a natural cutoff (of the order of the inverse size of the emitting system, e.g., the Bohr radius for an atom), that can be explicitly evaluated and determines the range of the atomic or molecular form factor (Berestetskii, Lifshits and Pitaevskii [1982], Moses [1972a,b, 1973], Seke [1994a,b]).

In order to scale the quantity B, we take the limit of a very large cavity, by keeping the density of Ω_0-photons in the cavity constant:

$$V \to \infty, \qquad \bar{N}_0 \to \infty, \quad \text{with} \quad \frac{\bar{N}_0}{V} = n_0 = \text{const.}, \tag{9.21}$$

and obtain from (9.17)

$$B^2 = n_0 V |\Phi_{k_0\lambda_0}|^2 = (2\pi)^3 n_0 |\varphi_{\lambda_0}(\boldsymbol{k}_0)|^2, \tag{9.22}$$

where $\varphi \equiv \Phi V^{1/2}/(2\pi)^{3/2}$ is the scaled matrix element of the 1–3 transition. If the 1–3 transition is of the dipole type, the above formula reads

$$B^2 = 2\pi\alpha\Omega_0 |\boldsymbol{\epsilon}^*_{k_0\lambda_0} \cdot \boldsymbol{x}_{13}|^2 n_0, \tag{9.23}$$

where $\boldsymbol{x}_{13}$ is the dipole matrix element.

In terms of laser power P and laser spot area A, eq. (9.23) reads

$$B^2 = \frac{P}{cA}\frac{\lambda_L^3}{16\pi^2}(\hbar\Gamma_{13}) = 132\frac{P\lambda_L^3}{A}(\hbar\Gamma_{13})\ \mathrm{eV}^2, \tag{9.24}$$

where P is expressed in watt, λ_L (laser wavelength) in μm, A in μm^2 and $\hbar\Gamma_{13}$ in eV. In eq. (9.24) the quantity B is expressed in suitable units and can be

easily compared to ω_0 (the ratio B/ω_0 being the relevant quantity, as we shall see). For laser intensities that are routinely used in the study of electromagnetic induced transparency, the inverse quantum Zeno effect should be experimentally observable. For a quick comparison remember that B is just half the Rabi frequency of the resonant transition 1–3.

9.3. *Laser off*

Let us first look at the case $B = 0$. The laser is off and we expect to recover the well-known physics of the spontaneous emission of a two-level system prepared in an excited state and coupled to the vacuum of the radiation field. In this case the self-energy function $\Sigma(0, E)$ reads, in the continuum limit (see eq. 8.9),

$$\Sigma(E) \equiv g^2\omega_0 q(E) \equiv g^2\omega_0 \int_0^\infty \mathrm{d}\omega \, \frac{\chi^2(\omega)}{E-\omega}, \tag{9.25}$$

where χ is defined in (9.18). The function $\tilde{x}(E)$ in eq. (9.13) (with $B = 0$) has a logarithmic branch cut, extending from 0 to $+\infty$, and no singularities on the first Riemann sheet (physical sheet) (Facchi and Pascazio [1998]). On the other hand, it has a simple pole on the second Riemann sheet, that is the solution of the equation

$$E - \omega_0 - g^2\omega_0 q_{\mathrm{II}}(E) = 0, \tag{9.26}$$

where

$$q_{\mathrm{II}}(E) = q(E\mathrm{e}^{-2\pi i}) = q(E) - 2\pi i\chi^2(E) \tag{9.27}$$

is the determination of $q(E)$ on the second Riemann sheet. We note that $g^2 q(E)$ is $\mathrm{O}(g^2)$, so that the pole can be found perturbatively. By expanding $q_{\mathrm{II}}(E)$ around ω_0 we get a power series, whose radius of convergence is $R_c = \omega_0$ because of the branch point at the origin. The circle of convergence lies half on the first Riemann sheet and half on the second sheet (fig. 19). The pole is well inside the convergence circle, because $|E_{\mathrm{pole}} - \omega_0| \sim g^2\omega_0 \ll R_c$, and we can write

$$E_{\mathrm{pole}} = \omega_0 + g^2\omega_0 q_{\mathrm{II}}(\omega_0 - \mathrm{i}0^+) + \mathrm{O}(g^4) = \omega_0 + g^2\omega_0 q(\omega_0 + i0^+) + \mathrm{O}(g^4), \tag{9.28}$$

because $q_{\mathrm{II}}(E)$ is the analytic continuation of $q(E)$ below the branch cut. By setting

$$E_{\mathrm{pole}} = \omega_0 + \Delta - \mathrm{i}\frac{\gamma}{2}, \tag{9.29}$$

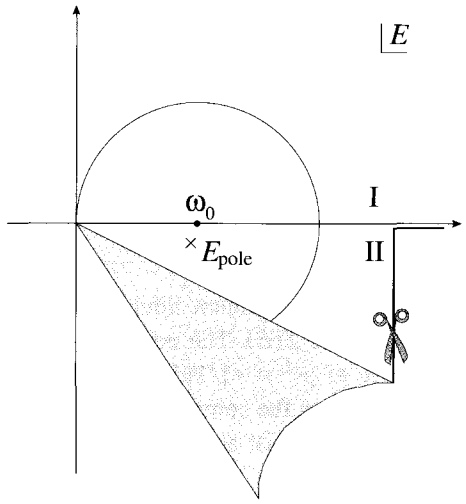

Fig. 19. Cut and pole in the E-plane ($B = 0$) and convergence circle for the expansion of $\Sigma(E)$ around $E = \omega_0$. I and II are the first and second Riemann sheets, respectively. The pole is on the second Riemann sheet, at a distance $\mathrm{O}(g^2)$ from ω_0.

one obtains from eq. (9.25)

$$\gamma = 2\pi g^2\omega_0\chi^2(\omega_0) + \mathrm{O}(g^4), \qquad \Delta = g^2\omega_0 P\int_0^\infty d\omega \, \frac{\chi^2(\omega)}{\omega_0 - \omega} + \mathrm{O}(g^4), \tag{9.30}$$

which are the Fermi "golden rule" and the second-order correction to the energy of level $|2\rangle$ (see eqs. 8.19).

The Weisskopf–Wigner approximation consists in neglecting all branch cut contributions and approximating the self-energy function with a constant (its value in the pole), that is

$$\tilde{x}(E) = \frac{\mathrm{i}}{E - \omega_0 - \Sigma(E)} \simeq \frac{\mathrm{i}}{E - \omega_0 - \Sigma_{\mathrm{II}}(E_{\mathrm{pole}})} = \frac{\mathrm{i}}{E - E_{\mathrm{pole}}}, \tag{9.31}$$

where in the last equality we used the pole equation (9.26). This yields a purely exponential behavior, $x(t) = \exp(-\mathrm{i}E_{\mathrm{pole}}t)$, without short-time (and long-time) corrections. As is well known, the latter are all contained in the neglected branch cut contribution.

9.4. *Laser on*

We now turn our attention to the situation with the laser switched on ($B \neq 0$) and tuned at the 1–3 transition frequency Ω_0. The self-energy function $\Sigma(B, E)$

in (9.16) depends on B and can be written in terms of the self-energy function $\Sigma(E)$ in absence of the laser field (eq. 9.25), by making use of the following remarkable property:

$$\Sigma(B,E) = \tfrac{1}{2}\sum_{k,\lambda} |\phi_{k\lambda}|^2 \left(\frac{1}{E-\omega_k-B} + \frac{1}{E-\omega_k+B}\right) = \tfrac{1}{2}\left[\Sigma(E-B)+\Sigma(E+B)\right]. \tag{9.32}$$

Notice, incidentally, that in the continuum limit ($V \to \infty$), due to the above formula, $\Sigma(B,E)$ scales just like $\Sigma(E)$. The position of the pole E_{pole} (and as a consequence the lifetime $\tau_E \equiv \gamma^{-1} = -1/2\text{Im}E_{\text{pole}}$) depends on the value of B. There are now two branch cuts in the complex E plane, due to the two terms in eq. (9.32). They lie over the real axis, along $[-B,+\infty)$ and $[+B,+\infty)$.

The pole satisfies the equation

$$E - \omega_0 - \Sigma(B,E) = 0, \tag{9.33}$$

where $\Sigma(B,E)$ is of order g^2, as before, and can again be expanded in a power series around $E = \omega_0$, in order to find the pole perturbatively. However, this time one has to choose the right determination of the function $\Sigma(B,E)$. Two cases are possible: (a) The branch point $+B$ is situated at the left of ω_0, so that ω_0 lies on both cuts; see fig. 20a. (b) The branch point $+B$ is situated at the right of ω_0, so that ω_0 lies only on the upper branch cut; see fig. 20b. We notice that in the latter case ($B > \omega_0$) a number of additional effects should be considered. Multi-photon processes would take place, the other atomic levels would start to play an important role and our approach (3-level atom in the rotating wave approximation) would no longer be completely justified. Notice also that our approximation still applies for values of B that are of the same order of magnitude as those utilized in the electromagnetic-induced transparency. In this case the influence of the other atomic levels can be taken into account and does not modify the main conclusions (Facchi and Pascazio [2000]).

In case (a), i.e., for $B < \omega_0$, the pole is on the third Riemann sheet (under both cuts) and the power series converges in a circle lying half on the first and half on the third Riemann sheet, within a convergence radius $R_c = \omega_0 - B$, which decreases as B increases [fig. 20a]. On the other hand, in case (b), i.e., for $B > \omega_0$, the pole is on the second Riemann sheet (under the upper cut only) and the power series converges in a circle lying half on the first and half on the second Riemann sheet, within a convergence radius $R_c = B - \omega_0$, which increases with B (fig. 20b).

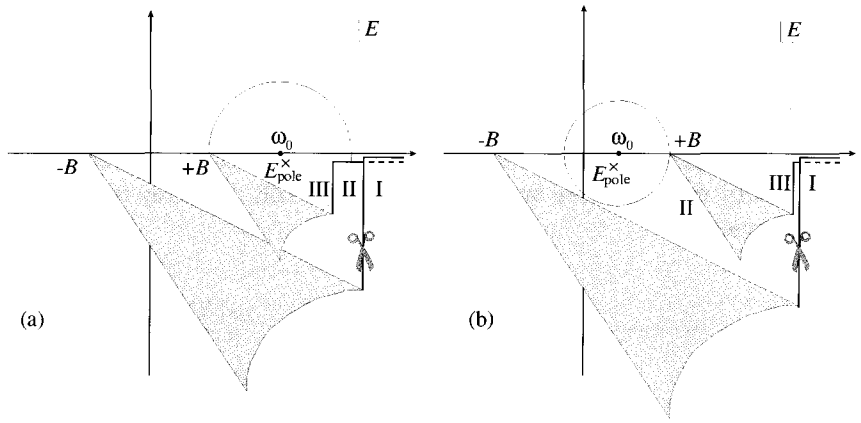

Fig. 20. Cuts and pole in the E-plane ($B \neq 0$) and convergence circle for the expansion of $\Sigma(B,E)$ around $E = \omega_0$. I, II and III are the first, second and third Riemann sheets, respectively. (a) $B < \omega_0$. (b) $B > \omega_0$. In both cases, the pole is at a distance $O(g^2)$ from ω_0.

In either cases we obtain, for $|E_{\text{pole}} - \omega_0| < R_c = |B - \omega_0|$,

$$E_{\text{pole}} = \omega_0 + \tfrac{1}{2}\left[\Sigma(\omega_0+B+i0^+) + \Sigma(\omega_0-B+i0^+)\right] + O(g^4) = \omega_0 + \tfrac{1}{2}g^2\omega_0\left[q(\omega_0+B+i0^+) + q(\omega_0-B+i0^+)\right] + O(g^4). \tag{9.34}$$

We write, as in eq. (9.29),

$$E_{\text{pole}} = \omega_0 + \Delta(B) - i\frac{\gamma_{\text{eff}}(B)}{2}. \tag{9.35}$$

Substituting (9.25) into (9.34) and taking the imaginary part, one obtains the following expression for the decay rate

$$\gamma_{\text{eff}}(B) = \pi g^2\omega_0\left[\chi^2(\omega_0+B) + \chi^2(\omega_0-B)\theta(\omega_0-B)\right] + O(g^4), \tag{9.36}$$

which yields, by (9.30),

$$\gamma_{\text{eff}}(B) = \gamma\,\frac{\chi^2(\omega_0+B) + \chi^2(\omega_0-B)\theta(\omega_0-B)}{2\chi^2(\omega_0)} + O(g^4). \tag{9.37}$$

Equation (9.37) expresses the "new" lifetime $\gamma_{\text{eff}}(B)^{-1}$, when the system is bathed in an intense laser field B, in terms of the "ordinary" lifetime γ^{-1}, when there is no laser field. By taking into account the general behavior (9.19) of the matrix elements $\chi^2(\omega)$ and substituting into (9.37), one gets to $O(g^4)$

$$\gamma_{\text{eff}}(B) \simeq \frac{\gamma}{2}\left[\left(1+\frac{B}{\omega_0}\right)^{2j\mp1} + \left(1-\frac{B}{\omega_0}\right)^{2j\mp1}\theta(\omega_0-B)\right] \quad (B \ll \Lambda), \tag{9.38}$$

where $\mp$ refers to 1–2 transitions of electric and magnetic type, respectively. Observe that, since Λ ~ inverse Bohr radius, the case $B < \omega_0 \ll \Lambda$ is the

physically most relevant one. The decay rate is profoundly modified by the presence of the laser field. Its behavior is shown in fig. 21 for a few values of j. In general, for $j > 1$ (1–2 transitions of electric quadrupole, magnetic dipole or higher), the decay rate $\gamma_{\rm eff}(B)$ increases with B, so that the lifetime $\gamma_{\rm eff}(B)^{-1}$ decreases as B is increased. Since B is the strength of the observation performed by the laser beam on level $|2\rangle$, this is an IZE, for decay is *enhanced* by observation.

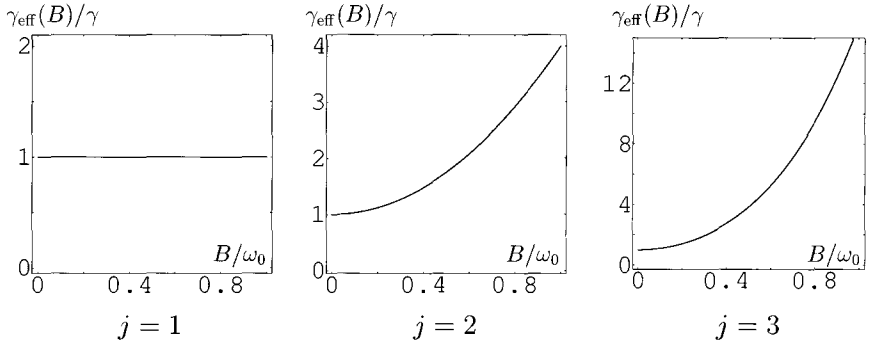

Fig. 21. The decay rate $\gamma_{\rm eff}(B)$ versus B, for electric transitions with $j = 1, 2, 3$; $\gamma_{\rm eff}(B)$ is in units γ and B is in units ω_0. Notice the different scales on the vertical axis.

As already emphasized, eq. (9.38) is valid for $B \ll \Lambda$. In the opposite case $B \gg \Lambda$, by (9.19) and (9.37), one gets to $O(g^4)$

$$\gamma_{\rm eff}(B) \simeq \frac{\gamma}{2}\,\frac{\chi^2(B)}{\chi^2(\omega_0)} \propto (B/\Lambda)^{-\beta}. \qquad (B \gg \Lambda) \tag{9.39}$$

This result is similar to that obtained by Mihokova, Pascazio and Schulman [1997]. If such high values of B were experimentally obtainable, the decay would be considerably hindered (QZE).

A final remark is now in order. If one would use the Weisskopf–Wigner approximation (9.31) in eq. (9.32), in order to evaluate the new lifetime, by setting $\Sigma(E) = \Sigma(E_{\rm pole}) = \text{const}$, one would obtain $\Sigma(B,E) = \Sigma(E) = \Sigma(E_{\rm pole})$, i.e., no B-dependence. Therefore, the effect we are discussing is ultimately due to the nonexponential contributions arising from the cut. In particular, viewed from the perspective of the time domain, this effect is ascribable to the quadratic short-time behavior of the $|2\rangle \to |1\rangle$ decay.

9.5. *Photon spectrum, dressed states and induced transparency*

It is interesting to look at the spectrum of the emitted photons. It is easy to check that, in the Weisskopf–Wigner approximation, the survival probability $|x(t)|^2$ decreases exponentially with time. In this approximation, for any value of B, the spectrum of the emitted photons is Lorentzian. The proof is straightforward and is given in Facchi and Pascazio [2000]. One finds that, for $B = 0$, the probability to emit a photon in the range $(\omega, \omega + d\omega)$ reads

$$dP_{B=0} = g^2\omega_0\chi^2(\omega) f_{\rm L}(\omega - \bar\omega_0; \gamma)\, d\omega, \tag{9.40}$$

where $\bar\omega_0 = \omega_0 + \Delta(B)$ and

$$f_{\rm L}(\omega;\gamma) = \frac{1}{\omega^2 + \gamma^2/4}. \tag{9.41}$$

On the other hand, when $B \neq 0$ one gets:

$$dP_B = g^2\omega_0\chi^2(\omega)\tfrac{1}{2}\,[f_L(\omega - \bar\omega_0 - B; \gamma_{\rm eff}(B)) + f_L(\omega - \bar\omega_0 + B; \gamma_{\rm eff}(B))]\, d\omega. \tag{9.42}$$

The emission probability is given by the sum of two Lorentzians, centered in $\bar\omega_0 \pm B$. We see that the emission probability of a photon of frequency $\bar\omega_0 + B$ ($\bar\omega_0 - B$) increases (decreases) with B (fig. 22). The linewidths are modified according to eq. (9.38). When B reaches the "threshold" value $\bar\omega_0$, only the photon of higher frequency ($\bar\omega_0 + B$) is emitted (with increasing probability vs. B).

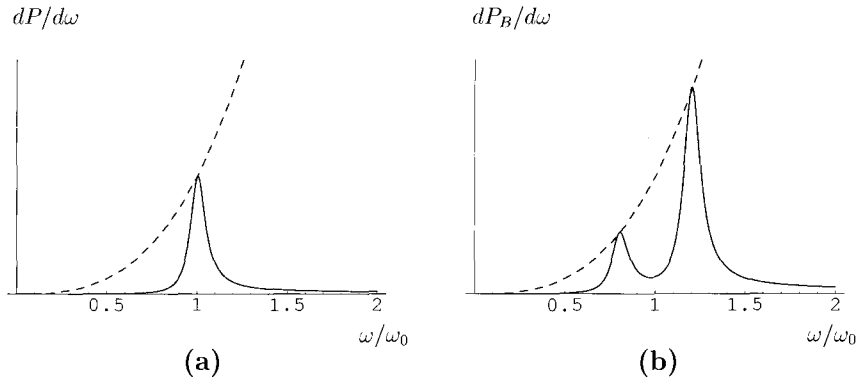

Fig. 22. The spectrum (9.42) of the emitted photons. The height of the Lorentzians is proportional to the matrix element $\chi^2(\omega)$ (dashed line). We chose an electric quadrupole transition, with $j = 2$ and $\gamma = 10^{-1}\bar\omega_0$, and used arbitrary units on the vertical axis. (a) $B = 0$; (b) $B = \bar\omega_0/5$; note that, from eq. (9.38), $\gamma_{\rm eff}(B) = (28/25)\gamma$.

Photons of different frequencies are therefore emitted at different rates. In order to understand better the features of the emission, let us look at the dressed states of the system. For simplicity, since the average number $\bar{N}_0$ of $\boldsymbol{k}_0$-photons in the total volume V can be considered very large, we consider number (rather than coherent) states of the electromagnetic field. Henceforth, the vector $|i; n_{k\lambda}, M_0\rangle$ represents an atom in state $|i\rangle$, with $n_{k\lambda}$ $(\boldsymbol{k}, \lambda)$-photons and M_0 laser photons.

The Hamiltonian (9.1) becomes

$$H \simeq \omega_0|2\rangle\langle 2| + \Omega_0|3\rangle\langle 3| + \sum_{k,\lambda} \omega_k a^\dagger_{k\lambda} a_{k\lambda} + \sum_{k,\lambda}{}' \left(\phi_{k\lambda} a^\dagger_{k\lambda}|1\rangle\langle 2| + \phi^*_{k\lambda} a_{k\lambda}|2\rangle\langle 1|\right) + \left(\Phi_{k_0\lambda_0} a^\dagger_{k_0\lambda_0}|1\rangle\langle 3| + \Phi^*_{k_0\lambda_0} a_{k_0\lambda_0}|3\rangle\langle 1|\right), \tag{9.43}$$

where a prime means that the summation does not include $(\boldsymbol{k}_0, \lambda_0)$ (due to hypothesis 9.3). Besides (9.6), there is now another conserved quantity: indeed the operator

$$\mathcal{N}_0 = |3\rangle\langle 3| + a^\dagger_{k_0\lambda_0} a_{k_0\lambda_0} \tag{9.44}$$

satisfies

$$[H, \mathcal{N}_0] = [\mathcal{N}_0, \mathcal{N}] = 0. \tag{9.45}$$

In this case, the system evolves in the subspace labeled by the two eigenvalues $\mathcal{N} = 1$ and $\mathcal{N}_0 = N_0$, whose states read

$$|\psi(t)\rangle = x(t)|2; 0, N_0\rangle + \sum_{k,\lambda}{}' y_{k\lambda}(t)|1; 1_{k\lambda}, N_0\rangle + \sum_{k,\lambda}{}' z_{k\lambda}(t)|3; 1_{k\lambda}, N_0 - 1\rangle. \tag{9.46}$$

By using the Hamiltonian (9.43) and the states (9.46) and identifying N_0 with $\bar{N}_0 = |\alpha_0|^2$ of § 9.1, the Schrödinger equation yields again the equations of motion (9.11), obtained by assuming a coherent state for the laser mode. Our analysis is therefore independent of the statistics of the driving field, provided it is sufficiently intense, and the (convenient) use of number states is completely justified.

Energy conservation implies that if there are two emitted photons with different energies (see eq. 9.42), there are two levels of different energies to which the atom can decay. This can be seen by considering the laser-dressed (Fano) atomic states (Fano [1961], Cohen-Tannoudji and Reynaud [1977a–c], Yoo and Eberly [1985]). The shift of the dressed states can be obtained directly

from the Hamiltonian (9.43). In the sector $\mathcal{N}_0 = N_0$, the operator $\mathcal{N}_0$ is proportional to the unit operator, the constant of proportionality being its eigenvalue. Hence one can write the Hamiltonian in the following form

$$H = H - \Omega_0 \mathcal{N}_0 + \Omega_0 N_0, \tag{9.47}$$

which, by the setting $E_1 + N_0\Omega_0 = 0$, reads

$$\begin{aligned} H &= H_0 + H_{\text{int}} \\ &= \omega_0|2\rangle\langle 2| + \sum_{k,\lambda}{}' \omega_k a^\dagger_{k\lambda} a_{k\lambda} + \sum_{k,\lambda}{}' \left(\phi_{k\lambda} a^\dagger_{k\lambda}|1\rangle\langle 2| + \phi^*_{k\lambda} a_{k\lambda}|2\rangle\langle 1|\right) \\ &\quad + \left(\Phi_{k_0\lambda_0} a^\dagger_{k_0\lambda_0}|1\rangle\langle 3| + \Phi^*_{k_0\lambda_0} a_{k_0\lambda_0}|3\rangle\langle 1|\right). \end{aligned} \tag{9.48}$$

On the other hand, in the sector $\mathcal{H}_{\mathcal{N}\mathcal{N}_0}$ with $\mathcal{N} = 1$ and $\mathcal{N}_0 = N_0$, the last term becomes

$$\left(\Phi_{k_0\lambda_0} a^\dagger_{k_0\lambda_0}|1\rangle\langle 3| + \Phi^*_{k_0\lambda_0} a_{k_0\lambda_0}|3\rangle\langle 1|\right) = \left(\Phi_{k_0\lambda_0}\sqrt{N_0}|1\rangle\langle 3| + \Phi^*_{k_0\lambda_0}\sqrt{N_0}|3\rangle\langle 1|\right). \tag{9.49}$$

This operator is easily diagonalized in terms of the (orthonormal) noninteracting states

$$|\pm\rangle = \frac{1}{\sqrt{2}}(|1\rangle + |3\rangle) \tag{9.50}$$

[this is the simplest choice (Facchi and Pascazio [2000])]. A simple manipulation yields

$$H = H'_0 + H'_{\text{int}}, \tag{9.51}$$

where the primed free and interaction Hamiltonians read, respectively,

$$\begin{aligned} H'_0 &= \omega_0|2\rangle\langle 2| + B|+\rangle\langle +| - B|-\rangle\langle -| + \sum_{k,\lambda}{}' \omega_k a^\dagger_{k\lambda} a_{k\lambda}, \\ H'_{\text{int}} &= \sum_{k,\lambda}{}' \left[\left(\frac{\phi_{k\lambda}}{\sqrt{2}} a^\dagger_{k\lambda}|+\rangle\langle 2| + \frac{\phi^*_{k\lambda}}{\sqrt{2}} a_{k\lambda}|2\rangle\langle +|\right)\right. \\ &\quad \left. + \left(\frac{\phi_{k\lambda}}{\sqrt{2}} a^\dagger_{k\lambda}|-\rangle\langle 2| + \frac{\phi^*_{k\lambda}}{\sqrt{2}} a_{k\lambda}|2\rangle\langle -|\right)\right] \end{aligned} \tag{9.52}$$

and $B^2 = |\Phi_{k_0\lambda_0}|^2 N_0$. The dressed states $|+\rangle$ and $|-\rangle$ have energies $+B$ and $-B$ and interact with state $|2\rangle$ with a coupling $\phi_{k\lambda}/\sqrt{2}$. Since $2B = \Omega_{\text{Rabi}}$ this is

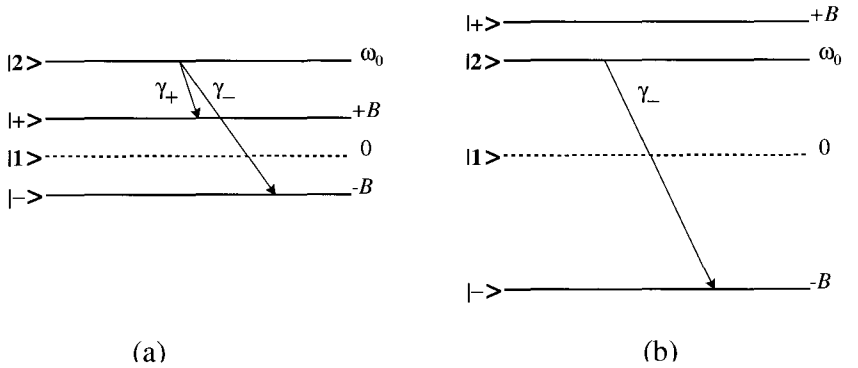

Fig. 23. Shift of the dressed states $|+\rangle$ and $|-\rangle$ vs. B. (a) For $B < \omega_0$ there are two decay channels, with $\gamma_- > \gamma_+$. (b) For $B > \omega_0$, level $|+\rangle$ is above level $|2\rangle$ and only the γ_- decay channel remains.

the well-known Autler–Townes doublet (Autler and Townes [1955], Townes and Schawlow [1975]).

Therefore, by applying the Fermi golden rule, the decay rates into the dressed states read

$$\gamma_+ = 2\pi g^2 \omega_0 \frac{\chi^2(\omega_0 - B)}{2}, \qquad \gamma_- = 2\pi g^2 \omega_0 \frac{\chi^2(\omega_0 + B)}{2}, \tag{9.53}$$

and the total decay rate of state $|2\rangle$ is given by their sum

$$\gamma_{\text{eff}}(B) = \gamma_+ + \gamma_-, \tag{9.54}$$

which yields (9.36). One sees why there is a threshold at $B = \omega_0$: For $B < \omega_0$, the energies of both dressed states $|\pm\rangle$ are lower than that of the initial state $|2\rangle$ (fig. 23a). The decay rate γ_- increases with B, whereas γ_+ decreases with B; their sum γ increases with B. These two decays (and their lifetimes) could be easily distinguished by selecting the frequencies of the emitted photons, e.g. by means of filters. On the other hand, when $B > \omega_0$, the energy of the dressed state $|+\rangle$ is larger than that of state $|2\rangle$ and this decay channel disappears (fig. 23b).

Finally, let us emphasize that if state $|2\rangle$ were *below* state $|1\rangle$, our system would become a three-level system in a ladder configuration, and the shift of the dressed states would give rise to electromagnetically induced transparency (Tewari and Agarwal [1986], Harris, Field and Imamoglu [1990], Boller, Imamoglu and Harris [1991], Field, Hahn and Harris [1991]). The situation we consider and the laser power required to bring these effects to light are therefore similar to those used in induced transparency.

For physically sensible values of the intensity of the laser field, the decay of level $|2\rangle$ is *faster* when the laser is present. Equations (9.37)–(9.38) (valid to 4th order in the coupling constant) express the new lifetime as a function of the "natural" one and other parameters characterizing the physical system. The initial state decays to the laser-dressed states with different lifetimes, yielding an IZE.

§ 10. Concluding remarks

The usual formulation of quantum Zeno effect in terms of repeated ("pulsed") measurements à la von Neumann is a very effective one. It motivated quite a few theoretical proposals and experiments and provoked very interesting discussions on their physical meaning. In general, the quantum Zeno effect is a straightforward consequence of the new dynamical features introduced by a series of measurement processes. In turn, a measurement process is due to the coupling with an external apparatus that, after interacting with the system, gets entangled with it.

It is then very natural to think that a quantum Zeno effect can also be obtained if the (Hamiltonian) dynamics is such that the interaction takes a sort of "close look" at the system. When such an interaction can be effectively described as a projection operator à la von Neumann, we obtain the usual formulation of the quantum Zeno effect in the limit of very frequent measurements. Otherwise, if the description in terms of projection operators does not apply, but one can still properly think in terms of a "continuous gaze" at the system, an explanation in terms of Zeno can still be very appealing and intuitive. These considerations and the diverse examples analyzed in this chapter motivated us to interpret several physical phenomena as quantum Zeno or inverse quantum Zeno effects.

We believe that this approach is prolific. Not only does it often yield a simple intuitive picture of the dynamical features of the system, it also enables one to look at these dynamical features from a different, new perspective. The very concept of inverse Zeno effect is a good example. Other examples are the phenomena discussed in §§ 7 and 9. The underlying idea is that coupling the system to an "observer" (like a laser) can sometimes enhance the evolution. This is close to Heraclitus' viewpoint, who used to argue (against Zeno and Parmenides) that everything flows. The physical features of the dynamical evolution laws have profound implications (Prigogine [1980]) and always provide matter for thoughts. In this way, one even finds links with instability (Facchi, Nakazato, Pascazio, Peřina and Řeháček [2001]), chaos (Facchi, Pascazio and

Scardicchio [1999], Kaulakys and Gontis [1997]) and geometrical phases (Berry and Klein [1996], Facchi, Klein, Pascazio and Schulman [1999]). The very fact that these links may not always be obvious is in itself a motivation to pursue the investigation in this direction.

Acknowledgments

It is a pleasure to thank the many colleagues who have collaborated with us during the last few years on the topics discussed in this chapter. We would like to mention in particular G. Badurek, Z. Hradil, A.G. Klein, H. Nakazato, M. Namiki, J. Peřina, H. Rauch, J. Řeháček, A. Scardicchio and L.S. Schulman. We owe them much of our own comprehension of the diverse phenomena known as Zeno effects.

References

Altenmuller, T.P., and A. Schenzle, 1994, Phys. Rev. A **49**, 2016.
Alvarez-Estrada, R.F., and J.L. Sánchez-Gómez, 1999, Phys. Lett. A **253**, 252.
Armstrong, L.A., N. Bloembergen, J. Ducuing and P.S. Pershan, 1962, Phys. Rev. **127**, 1918.
Autler, S.H., and C.H. Townes, 1955, Phys. Rev. **100**, 703.
Ballentine, L.E., 1991, Phys. Rev. A **43**, 5165.
Beige, A., and G. Hegerfeldt, 1996, Phys. Rev. A **53**, 53.
Berestetskii, V.B., E.M. Lifshits and L.P. Pitaevskii, 1982, Quantum Electrodynamics (Pergamon Press, Oxford) ch. 5.
Bernardini, C., L. Maiani and M. Testa, 1993, Phys. Rev. Lett. **71**, 2687.
Berry, M.V., 1995, in: Fundamental Problems in Quantum Theory, eds D.M. Greenberger and A. Zeilinger, Ann. N.Y. Acad. Sci. **755**, 303.
Berry, M.V., and S. Klein, 1996, J. Mod. Optics **43**, 165.
Beskow, A., and J. Nilsson, 1967, Ark. Fys. **34**, 561.
Blanchard, Ph., and A. Jadczyk, 1993, Phys. Lett. A **183**, 272.
Bloch, F., 1946, Phys. Rev. **70**, 460.
Boller, K.J., A. Imamoglu and S.E. Harris, 1991, Phys. Rev. Lett. **66**, 2593.
Breit, G., and E.P. Wigner, 1936, Phys. Rev. **49**, 519.
Chirkin, A.S., and V.V. Volkov, 1998, J. Russ. Laser Res. **19**, 409.
Cohen-Tannoudji, C., J. Dupont-Roc and G. Grynberg, 1998, Atom–Photon Interactions: Basic Processes and Applications (Wiley, New York).
Cohen-Tannoudji, C., and S. Reynaud, 1977a, J. Phys. B **10**, 345.
Cohen-Tannoudji, C., and S. Reynaud, 1977b, J. Phys. B **10**, 365.
Cohen-Tannoudji, C., and S. Reynaud, 1977c, J. Phys. B **10**, 2311.
Cook, R.J., 1988, Phys. Scripta T **21**, 49.
Dancoff, S., 1950, Phys. Rev. **78**, 382.
Facchi, P., A.G. Klein, S. Pascazio and L.S. Schulman, 1999, Phys. Lett. A **257**, 232.
Facchi, P., H. Nakazato and S. Pascazio, 2001, Phys. Rev. Lett. **86**, 2699.

Facchi, P., H. Nakazato, S. Pascazio, J. Peřina and J. Řeháček, 2001, Phys. Lett. A **279**, 117.
Facchi, P., and S. Pascazio, 1998, Phys. Lett. A **241**, 139.
Facchi, P., and S. Pascazio, 1999, Physica A **271**, 133.
Facchi, P., and S. Pascazio, 2000, Phys. Rev. A **62**, 023804.
Facchi, P., S. Pascazio and A. Scardicchio, 1999, Phys. Rev. Lett. **83**, 61.
Fano, U., 1961, Phys. Rev. **124**, 1866.
Fejer, M.M., G.A. Magel, D.H. Jundt and R.L. Byer, 1992, J. Quant. Electron. **28**, 26.
Fermi, E., 1932, Rev. Mod. Phys. **4**, 87.
Fermi, E., 1950, Nuclear Physics (University of Chicago Press, Chicago) pp. 136, 148.
Fermi, E., 1960, Notes on Quantum Mechanics. A Course Given at the University of Chicago in 1954, edited by E Segré (University of Chicago Press, Chicago) Lecture 23.
Feynman, R.P., F.L. Vernon Jr and R.W. Hellwarth, 1957, J. Appl. Phys. **28**, 49.
Field, J.E., K.H. Hahn and S.E. Harris, 1991, Phys. Rev. Lett. **67**, 3062.
Fock, V.A., and N.S. Krylov, 1947, J. Phys. **11**, 112.
Frerichs, V., and A. Schenzle, 1992, in: Foundations of Quantum Mechanics, eds T.D. Black, M.M. Nieto, H.S. Pilloff, M.O. Scully and R.M. Sinclair (World Scientific, Singapore) p. 59.
Gamow, G., 1928, Z. Phys. **51**, 204.
Gea-Banacloche, J., N. Lu, L.M. Pedrotti, S. Prasad, M.O. Scully and K. Wodkiewicz, 1990, Phys. Rev. A **41**, 381.
Ghirardi, G.C., C. Omero, T. Weber and A. Rimini, 1979, Nuovo Cim. A **52**, 421.
Harris, S.E., J.E. Field and A. Imamoglu, 1990, Phys. Rev. Lett. **64**, 1107.
Hellund, E.J., 1953, Phys. Rev. **89**, 919.
Home, D., and M.A.B. Whitaker, 1992, J. Phys. A **25**, 657.
Home, D., and M.A.B. Whitaker, 1993, Phys. Lett. A **173**, 327.
Home, D., and M.A.B. Whitaker, 1997, Ann. Phys. **258**, 237.
Hong, C.K., and L. Mandel, 1985, Phys. Rev. A **31**, 2409.
Hradil, Z., H. Nakazato, M. Namiki, S. Pascazio and H. Rauch, 1998, Phys. Lett. A **239** 333.
Huang, H., S.-Y. Zhu, M.S. Zubairy and M.O. Scully, 1996, Phys. Rev. A **53**, 1834.
Inagaki, S., M. Namiki and T. Tajiri, 1992, Phys. Lett. A **166**, 5.
Itano, W.H., D.J. Heinzen, J.J. Bollinger and D.J. Wineland, 1990, Phys. Rev. A **41**, 2295.
Itano, W.H., D.J. Heinzen, J.J. Bollinger and D.J. Wineland, 1991, Phys. Rev. A **43**, 5168.
Joichi, I., Sh. Matsumoto and M. Yoshimura, 1998, Phys. Rev. D **58**, 045004.
Kaulakys, B., and V. Gontis, 1997, Phys. Rev. A **56**, 1131.
Khalfin, L.A., 1957, Dokl. Acad. Nauk USSR **115**, 277 [Sov. Phys. Dokl. **2**, 340].
Khalfin, L.A., 1958, Zh. Eksp. Teor. Fiz. **33**, 1371 [Sov. Phys. JET **6**, 1053].
Khalfin, L.A., 1968, Zh. Eksp. Teor. Fiz. Pisma Red. **8**, 106 [JETP Letters **8**, 65].
Knight, P.L., and M.A. Lauder, 1990, Phys. Rep. **190**, 1.
Kofman, A.G., and G. Kurizki, 1996, Phys. Rev. A **54**, R3750.
Kofman, A.G., and G. Kurizki, 1999, Acta Phys. Slov. **49**, 541.
Kofman, A.G., and G. Kurizki, 2000, Nature **405**, 546.
Kraus, K., 1981, Found. Phys. **11**, 547.
Kwiat, P.G., H. Weinfurter, T.J. Herzog, A. Zeilinger and M. Kasevich, 1995, Phys. Rev. Lett. **74**, 4763.
Lang, R., M.O. Scully and W.E. Lamb Jr, 1973, Phys Rev. A **7**, 1778.
Ley, M., and R. Loudon, 1987, J. Mod. Opt. **34**, 227.
Luis, A., and J. Peřina, 1996, Phys. Rev. Lett. **76**, 4340.
Luis, A., and L.L. Sánchez-Soto, 1998, Phys. Rev. A **57**, 781.
Maiani, L., and M. Testa, 1998, Ann. Phys. New York **263**, 353.

Mandel, L., and E. Wolf, 1995, Optical Coherence and Quantum Optics (Cambridge University Press, Cambridge).
Mandelstam, L., and I. Tamm, 1945, J. Phys. **9**, 249.
Mihokova, E., S. Pascazio and L.S. Schulman, 1997, Phys. Rev. A **56**, 25.
Misra, B., and E.C.G. Sudarshan, 1977, J. Math. Phys. **18**, 756.
Mollow, B.R., 1975, Phys. Rev. A **12**, 1919.
Moses, H.E., 1972a, Lett. Nuovo Cim. **4**, 51.
Moses, H.E., 1972b, Lett. Nuovo Cim. **4**, 54.
Moses, H.E., 1973, Phys. Rev. A **8**, 1710.
Nakazato, H., M. Namiki and S. Pascazio, 1996, Int. J. Mod. Phys. B **10**, 247.
Nakazato, H., M. Namiki, S. Pascazio and H. Rauch, 1995, Phys. Lett. A **199**, 27.
Nakazato, H., M. Namiki, S. Pascazio and H. Rauch, 1996, Phys. Lett. A **217**, 203.
Namiki, M., and N. Mugibayashi, 1953, Prog. Theor. Phys. **10**, 474.
Namiki, M., S. Pascazio and H. Nakazato, 1997, Decoherence and Quantum Measurements (World Scientific, Singapore).
Pascazio, S., 1996, Quantum Zeno effect and inverse Zeno effect, in: Quantum Interferometry, eds F. De Martini, G. Denardo and Y. Shih (VCH, Weinheim) p. 525.
Pascazio, S., 1997, Found. Phys. **27**, 1655.
Pascazio, S., and P. Facchi, 1999, Acta Phys. Slov. **49**, 557.
Pascazio, S., and M. Namiki, 1994, Phys. Rev. A **50**, 4582.
Pascazio, S., M. Namiki, G. Badurek and H. Rauch, 1993, Phys. Lett. A **179**, 155.
Pati, A., 1996, Phys. Lett. A **215**, 7.
Peres, A., 1980, Am. J. Phys. **48**, 931.
Peres, A., and A. Ron, 1990, Phys. Rev. A **42**, 5720.
Petrosky, T., S. Tasaki and I. Prigogine, 1990, Phys. Lett. A **151**, 109.
Petrosky, T., S. Tasaki and I. Prigogine, 1991, Physica A **170**, 306.
Plenio, M.B., P.L. Knight and R.C. Thompson, 1996, Opt. Commun. **123**, 278.
Prigogine, I., 1980, From Being to Becoming (Freeman, New York).
Rabi, I.I., N.F. Ramsey and J. Schwinger, 1954, Rev. Mod. Phys. **26**, 167.
Radmore, P.M., and P.L. Knight, 1982, J. Phys. B **15**, 561.
Řeháček, J., J. Peřina, P. Facchi, S. Pascazio and L. Mišta, 2000, Phys. Rev. A **62**, 013804.
Saleh, B.E.A., and M.C. Teich, 1991, Fundamentals of Photonics (Wiley, New York) § 7.4.B.
Schulman, L.S., 1997, J. Phys. A **30**, L293.
Schulman, L.S., 1998, Phys. Rev. A **57**, 1509.
Schulman, L.S., A. Ranfagni and D. Mugnai, 1994, Phys. Scripta **49**, 536.
Seke, J., 1994a, Physica A **203**, 269.
Seke, J., 1994b, Physica A **203**, 284.
Stich, M.L., and M. Bass, 1985, Laser Handbook (North-Holland, Amsterdam) ch. 4.
Tamm, I., 1945, J. Phys. USSR **9**, 449.
Tewari, S.P., and G.S. Agarwal, 1986, Phys. Rev. Lett. **56**, 1811.
Thun, K., and J. Peřina, 1998, Phys. Lett. A **249**, 363.
Townes, C.H., and A.L. Schawlow, 1975, Microwave Spectroscopy (Dover, New York).
Venugopalan, A., and R. Ghosh, 1995, Phys. Lett. A **204**, 11.
von Neumann, J., 1932, Die Mathematische Grundlagen der Quantenmechanik (Springer, Berlin). English translation by E.T. Beyer: Mathematical Foundation of Quantum Mechanics (Princeton University Press, Princeton, 1955). For the QZE, see in particular p. 195 of the German edition (p. 366 of the English translation).
Weisskopf, V., and E.P. Wigner, 1930a, Z. Phys. **63**, 54.
Weisskopf, V., and E.P. Wigner, 1930b, Z. Phys. **65**, 18.

Whitaker, M.A.B., 2000, Progr. Quant. Electron. **24**, 1.
Wigner, E.P., 1963, Am. J. Phys. **31**, 6.
Wilkinson, S.R., C.F. Bharucha, M.C. Fischer, K.W. Madison, P.R. Morrow, Q. Niu, B. Sundaram and M.G. Raizen, 1997, Nature **387**, 575.
Yariv, A., and P. Yeh, 1984, Optical Waves in Crystals (Wiley, New York).
Yoo, H.-I., and J.H. Eberly, 1985, Phys. Rep. **118**, 239.
Zhu, S.-Y., L.M. Narducci and M.O. Scully, 1995, Phys. Rev. A **52**, 4791.
Zhu, S.-Y., and M.O. Scully, 1996, Phys. Rev. Lett. **76**, 388.